WAVELETS AND STRUCTURAL CHANGE

by D.S.G. POLLOCK

University of Leicester

Econometric models have traditionally depended of linear time-invariant structures. Structural changes have been accommodated by postulating structural breaks in which one locally invariant structure is succeeded by another, or by allowing for instantaneous switching between alternative regimes.

To accommodate structural changes of a more varied nature, it is appropriate to pursue a wavelets analysis.

In a wavelets analysis, a temporal data sequence is decomposed into its frequency-specific components, of which the amplitudes can vary through time. Thus, a wavelets analysis reveals the structure of the data in both its time and its frequency dimensions.

Spectral Structures in Econometric Data

The aggregate temporal structure can be revealed by the time plot of the data. The aggregate frequency composition of the data is revealed by the periodogram.

The periodogram is the plot of the squared amplitude coefficients $\rho_j^2 = \alpha_j^2 + \beta_j^2; j = 0, 1, \ldots, [T/2]$ derived from the Fourier decomposition of the data sequence $x_0, x_1, \ldots, x_{T-1}$, whereby the data are represented in terms of trigonometric functions:

$$x_t = \alpha_0 + \sum_{j=1}^{[T/2]} \{\alpha_j \cos(\omega_j t) + \beta_j \sin(\omega_j t)\}\,.$$

Here, $[T/2]$ is the integral part of $T/2$. The frequency values $\omega_j = 2\pi j/T; j = 0, 1, \ldots, [T/2]$ are equally spaced in the interval $[0, \pi]$. There are as many Fourier coefficients α_j, β_j as there are data points.

In order to decompose the data into frequency-specific components, an appropriate set of frequency bands must be determined. The bands can be determined in view of the periodogram of the data.

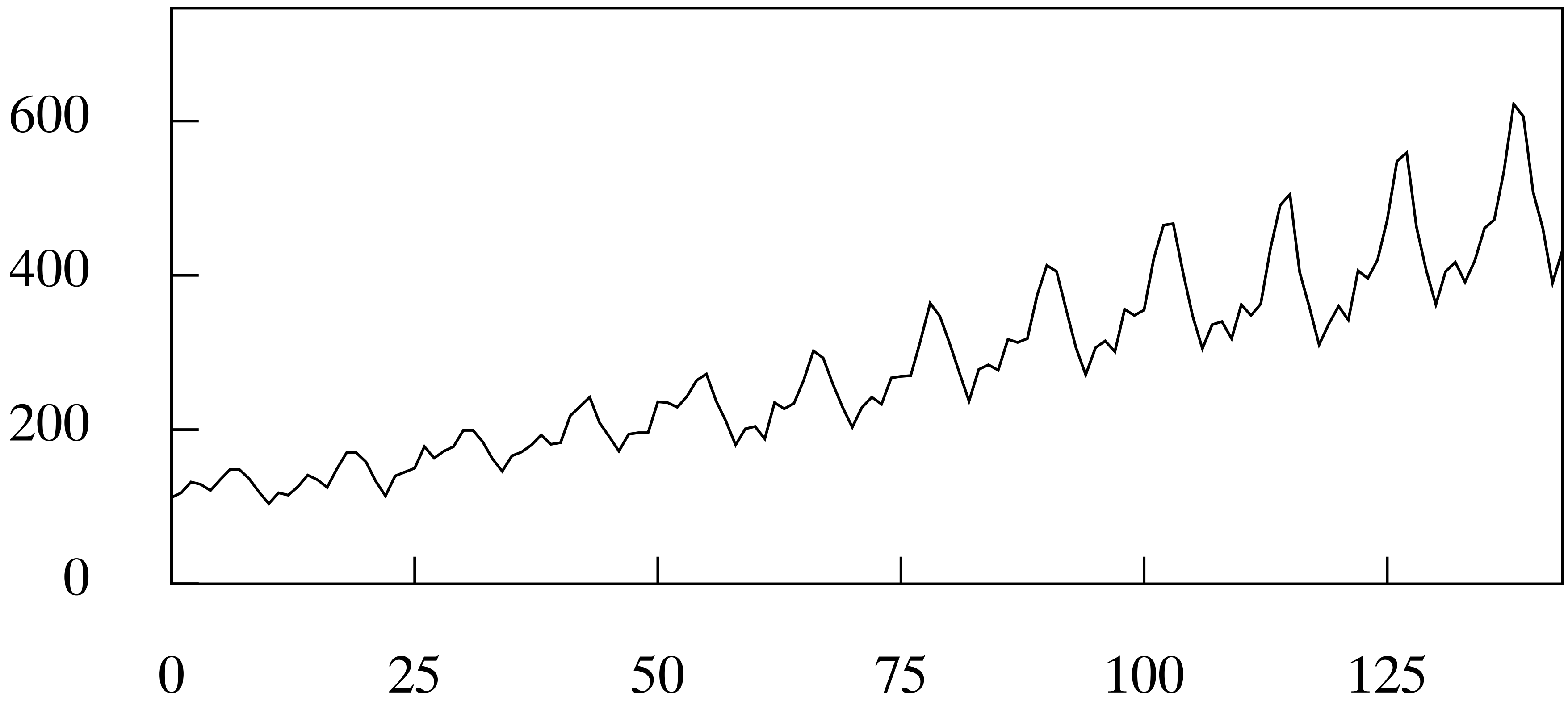

Figure 1. International airline passengers: monthly totals (thousands of passengers) January 1949–December 1960: 144 observations.

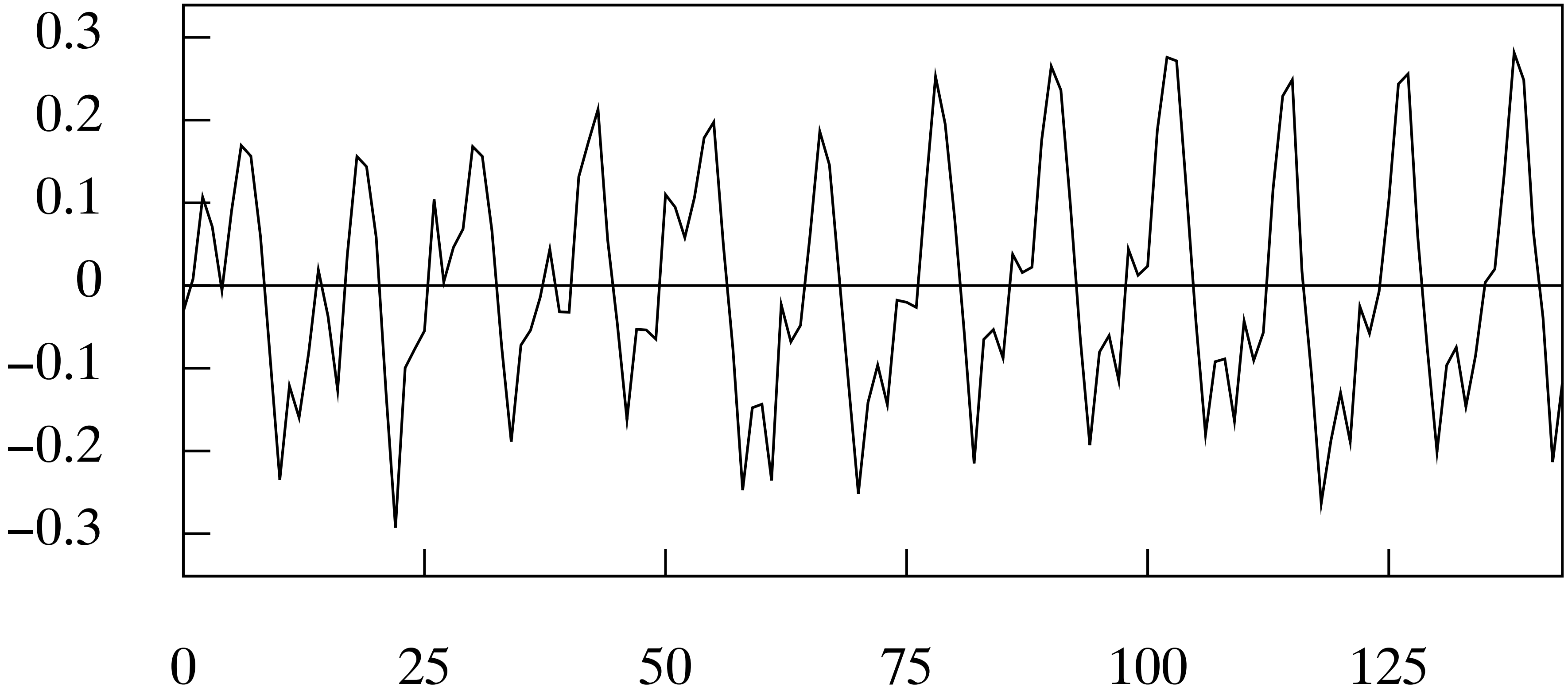

Figure 2. The seasonal fluctuation in the airline passenger series, represented by the residuals from fitting a quadratic function to the logarithms of the series.

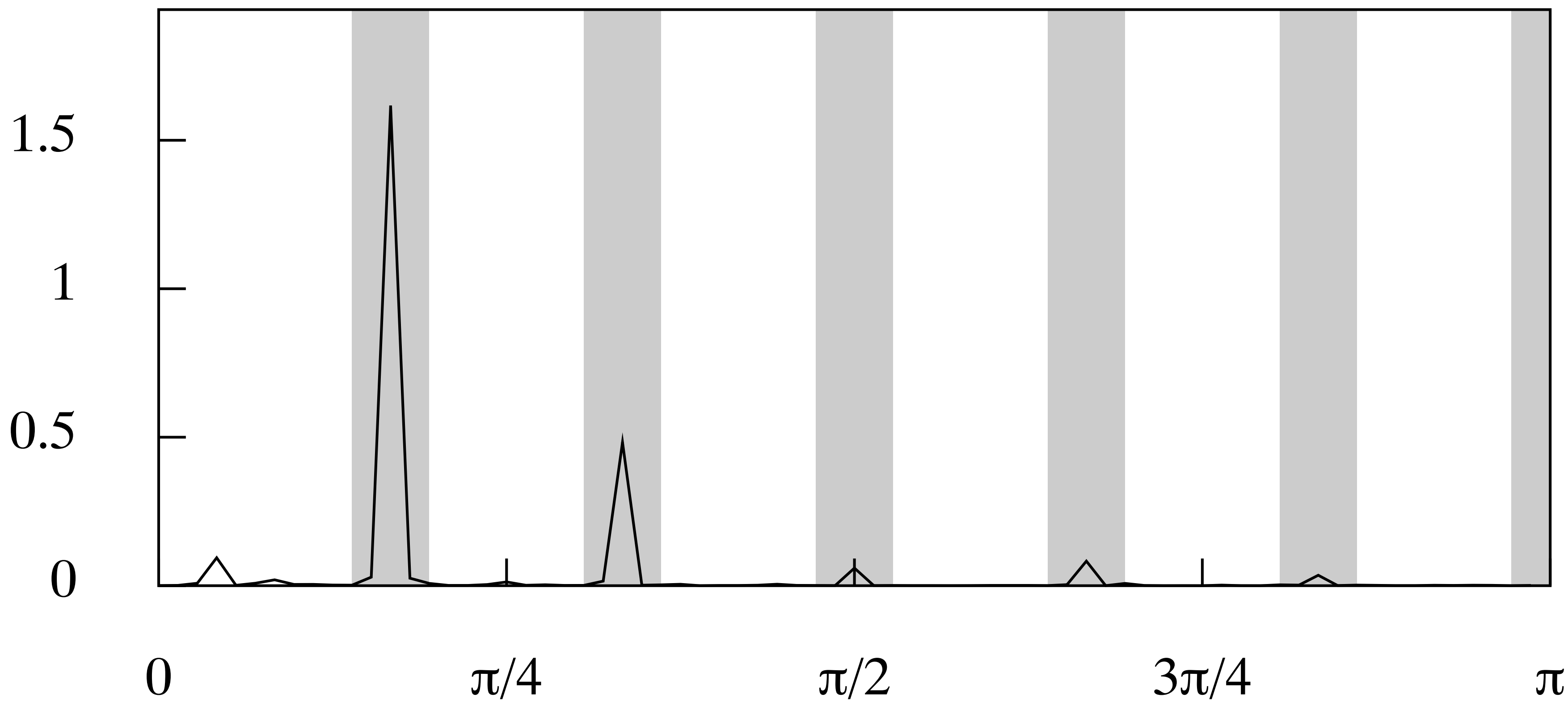

Figure 3. The periodogram of the seasonal fluctuations in the airline passenger series.

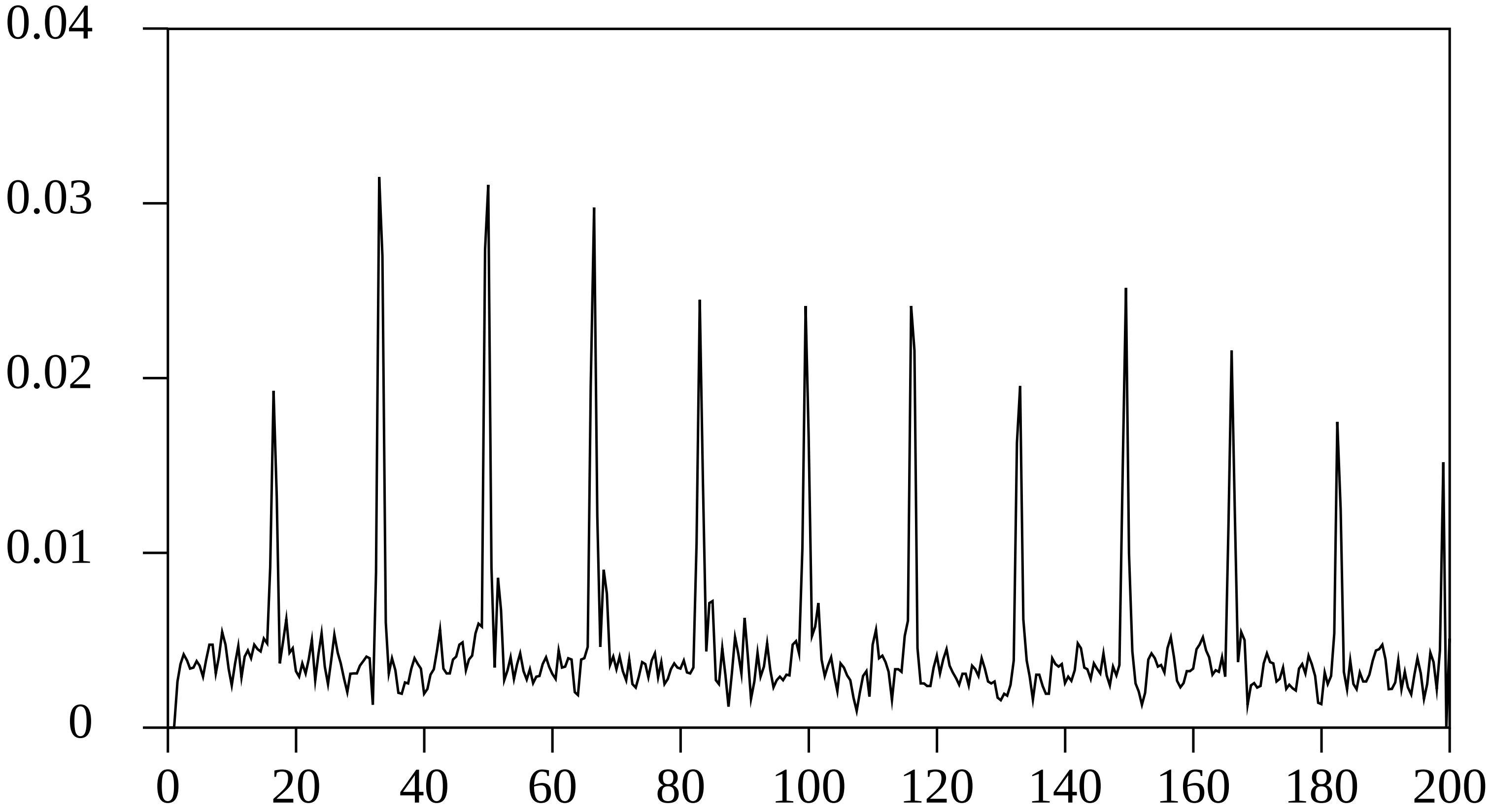

Figure 4. The power spectrum of the vibrations transduced from the casing of an electric motor in the process of a routine maintenance inspection. The units of the horizontal axis are hertz. The first peak at 16.6 hertz corresponds to a shaft rotation speed of 1000 rpm. The prominence of its successive harmonics corresponds to the rattling of a loose shaft.

The Fourier Analsysis of the Data:

According to the Shannon–Nyquist sampling theorem, given an appropriate rate of sampling, a continuous signal $x(t)$ with $t \in [0, T]$ that is limited to the frequency interval $[0, \pi]$ can be represented completely by a set of sampled ordinates $x_0, x_1, \ldots, x_{T-1}$. Thus

$$x(t) = \sum_{j=0}^{T-1} \xi_j e^{\mathrm{i}\omega_j t} = \sum_{j=0}^{[T/2]} \{\alpha_j \cos(\omega_j t) + \beta_j \sin(\omega_j t)\},$$

where $\xi_j = (\alpha_j - \mathrm{i}\beta_j)/2$ and $\xi_{-j} = (\alpha_j + \mathrm{i}\beta_j)/2$.

In that case, the Fourier ordinates ξ_j are from the discrete Fourier transform of T points sampled in the time domain, and there is

$$x(t) = \sum_{j=0}^{T-1} \xi_j e^{\mathrm{i}\omega_j t} \longleftrightarrow \xi_j = \frac{1}{T} \sum_{t=0}^{T-1} x_t e^{-\mathrm{i}\omega_j t}.$$

Trigonometric Functions and Sinc Functions

Putting the expressions for the Fourier ordinates into the finite Fourier series expansion of the time function and commuting the summation signs gives

$$x(t) = \sum_{j=0}^{T-1} \left\{ \frac{1}{T} \sum_{k=0}^{T-1} x_k e^{\mathrm{i}\omega_j k} \right\} e^{\mathrm{i}\omega_j t} = \frac{1}{T} \sum_{k=0}^{T-1} x_k \sum_{j=0}^{T-1} e^{\mathrm{i}\omega_j (t-k)}.$$

The inner summation gives rise to the Dirichlet Kernel:

$$\phi_n^{\circ}(t) = \sum_{t=0}^{T-1} e^{\mathrm{i}\omega_j t} = \frac{\sin([n - 1/2]\omega_1 t)}{\sin(\omega_1 t/2)}.$$

Thus, the Fourier expansion can be expressed in terms of the Dirichlet kernel, which is a circularly wrapped sinc function:

$$x(t) = \frac{1}{T} \sum_{t=0}^{T-1} x_k \phi_n^{\circ}(t - k).$$

Sinc Function and the Dirichlet Kernels

The Dirichlet kernel is a periodic function that is supported on the circumference of a circle of length T. The sinc function is the limiting case of the Dirichlet kernel as $T \to \infty$. We may analyse the sinc function in lieu of the kernel.

The sinc function is the Fourier transform of the square function $\phi(\omega)$ supported on the frequency interval $[-\pi, \pi]$:

$$\phi(t) = \frac{1}{2\pi} \int_{-\pi}^{\pi} e^{\mathrm{i}\omega} d\omega = \frac{\sin(\omega t)}{\pi t}.$$

Sampling this function at the integer points gives the discrete unit impulse function $\delta(t)$. The set of impulse functions $\{\delta(t-j); j = 0, \pm 1, \pm 2, \ldots\}$ at unit displacements forms a basis for temporal sequences. The sinc function at unit displacements forms a basis for continuous functions limited to the frequency interval $[0, \pi]$.

The condition $\phi(\omega) = \phi^2(\omega)$, which is the idempotency of the frequency-domain function, implies that the time-domain sinc function $\phi(t)$ is its own autocorrelation function: sinc functions at unit displacements are *sequentially* othogonal.

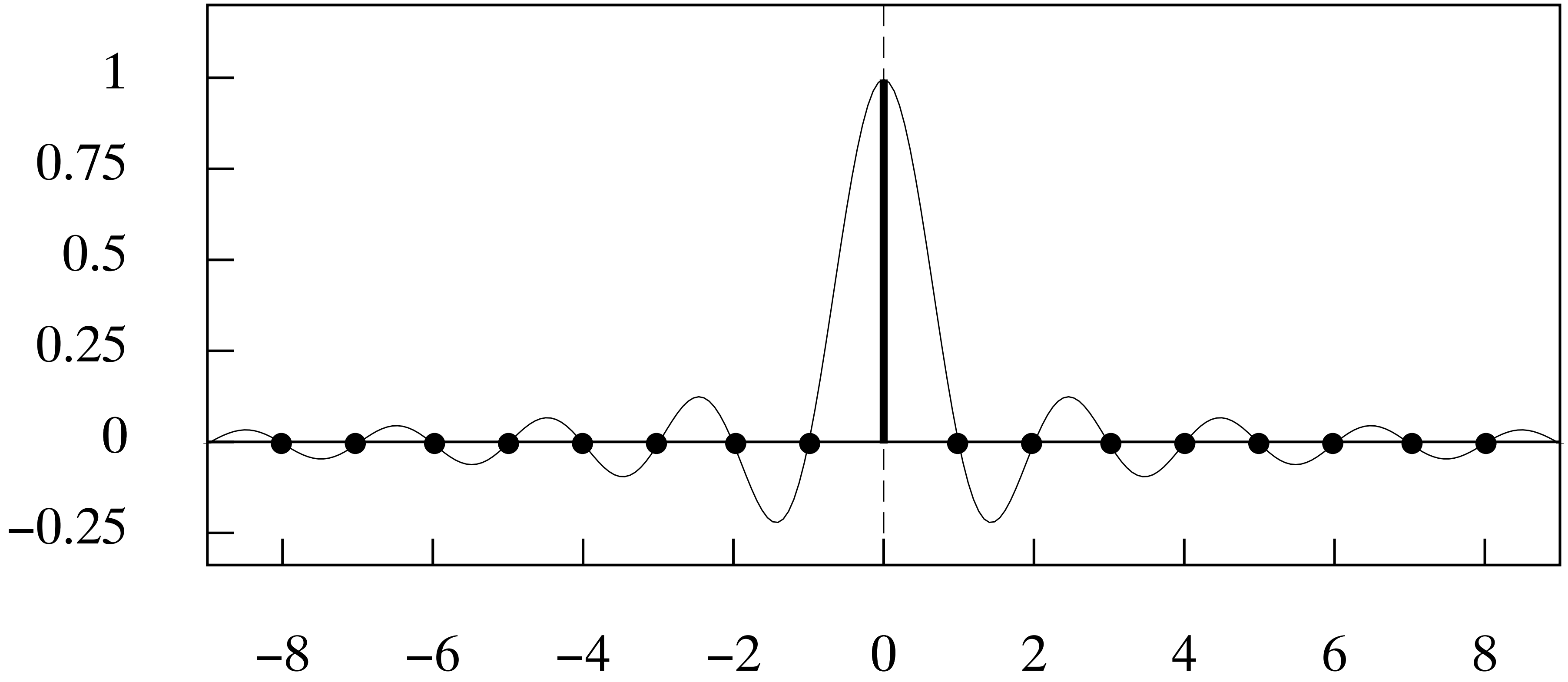

Figure 5. The sinc function $\phi(t)$.

Shannon Wavelet and Scaling Functions

The basis of sinc functions at unit displacements can be replaced by a combined basis of scaling functions $\phi_{(1)}(t-2j)$ and wavelets $\psi_{(1)}(t-2j)$ that reside within the frequency bands $[0, \pi/2]$ and $[\pi/2, \pi]$. These are displaced versions of

$$\phi_{(1)}(t) = \frac{\sin(\pi t/2)}{\pi t} \quad \text{and} \quad \psi_{(1)}(t) = \frac{\sin(\pi t) - \sin(\pi t/2)}{\pi t}$$
$$= \frac{2}{\pi t}\cos(3\pi t/4)\sin(\pi t/4).$$

The displacements are by two sample intervals; and the functions are both *laterally* and *sequentially* orthogonal.

More generally, a set of functions that span the frequency interval $[\alpha, \beta]$ is provided by displaced versions of the function

$$\psi(t) = \frac{1}{\pi t}\{\sin(\beta t) - \sin(\alpha)\} = \frac{2}{\pi t}\cos\{(\alpha+\beta)t/2\}\sin\{(\beta-\alpha)t/2\}$$
$$= \frac{2}{\pi t}\cos(\gamma t)\sin(\delta t),$$

where $\gamma = (\alpha + \beta)/2$ is the centre of the pass band and $\delta = (\beta - \alpha)/2$ is half its width.

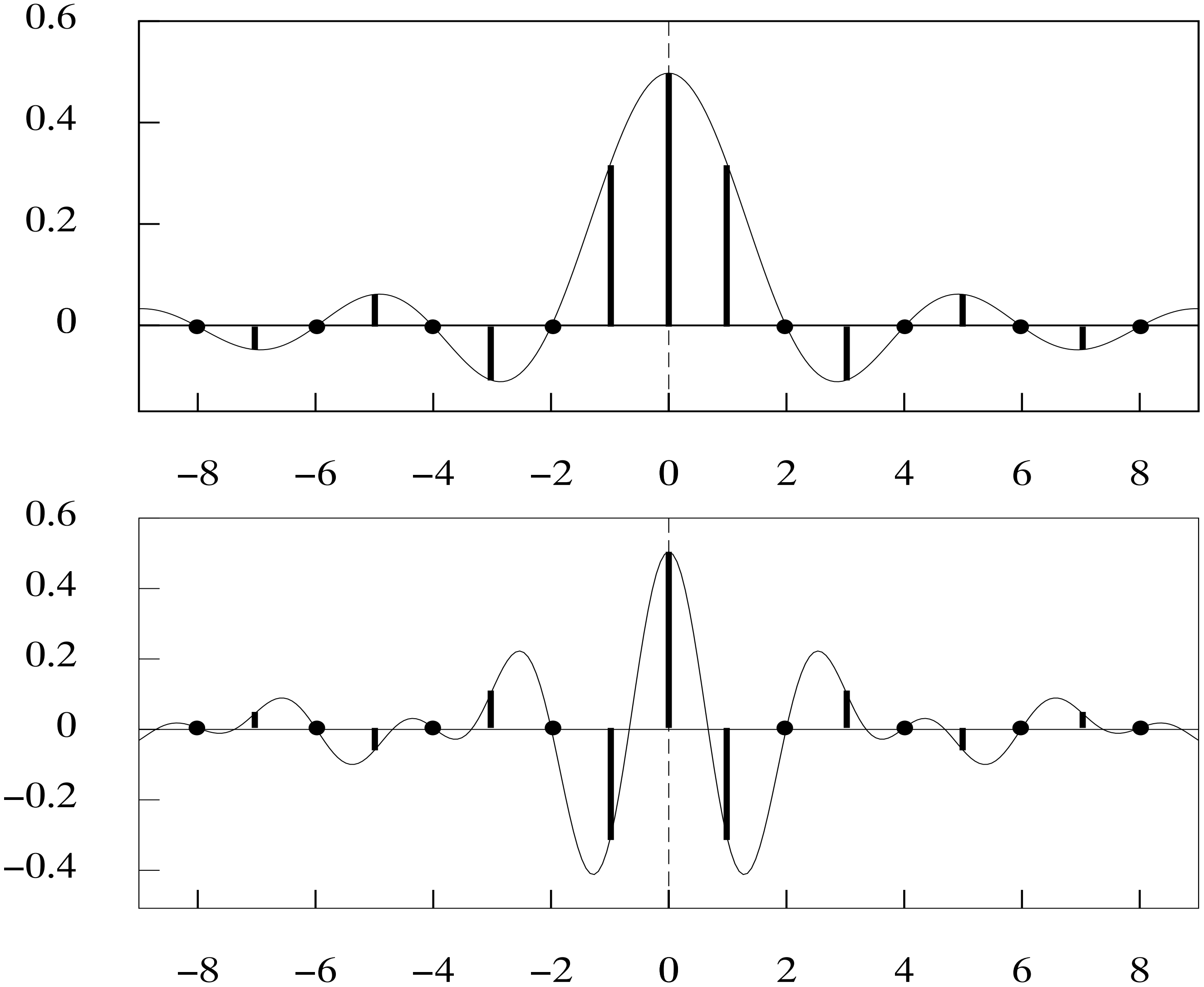

Figure 6. The scaling function $\phi_{(1)}(t)$ (top) and the wavelet function $\psi_{(1)}(t)$.

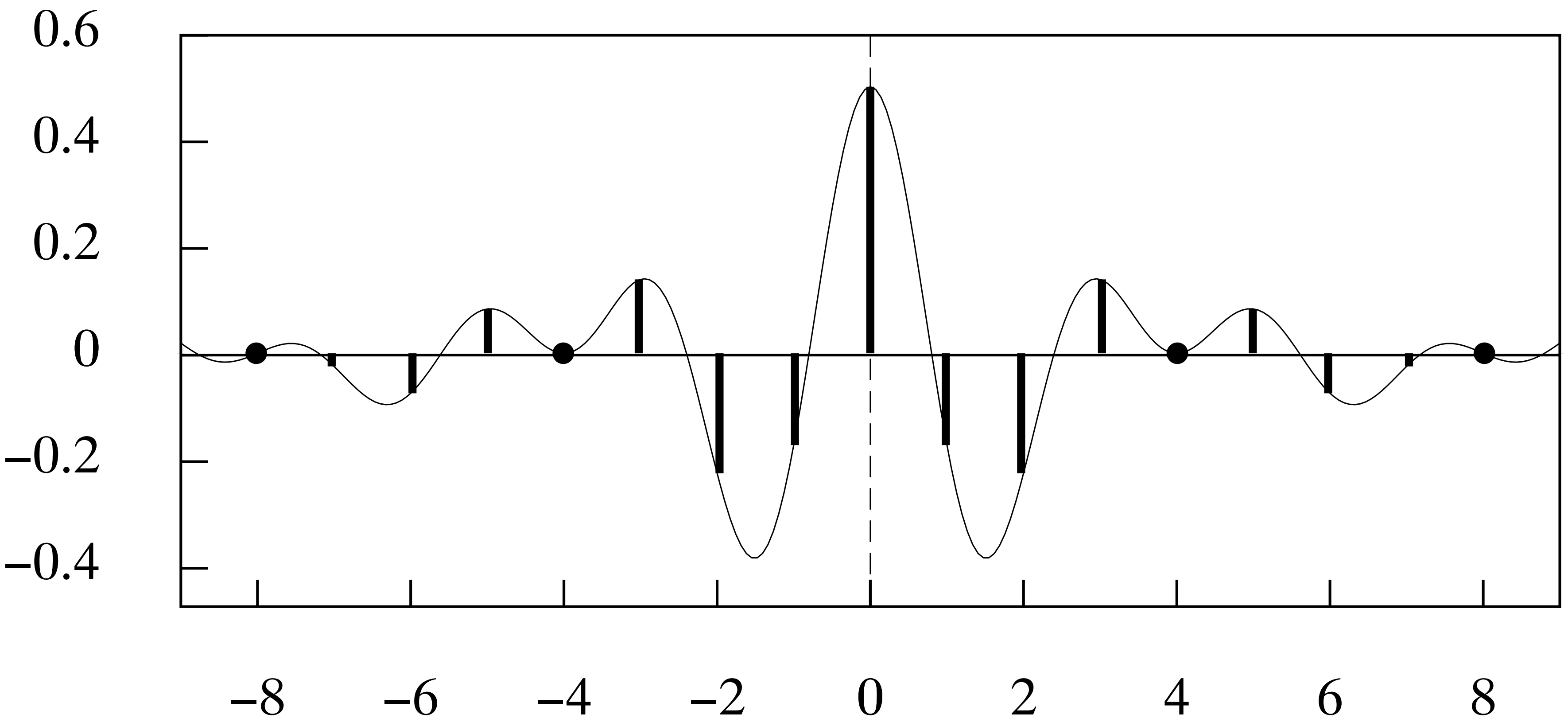

Figure 7. A wavelet within a frequency band of width $\pi/2$ running from $3\pi/8$ to $7\pi/8$.

Wavelets on Finite Supports

Shannon wavelets are supported on a doubly-infinite interval, and they converge slowly.

The problem of an infinite support may be overcome by circular wrapping, which is the result of sampling in the frequency domain.

The problem of slow convergence may be overcome by defining wavelets on finite supports. Functions with a finite support are unbounded in frequency and, therefore, non-analytic.

The supports of the Daubechies wavelets have a width of only three sample intervals, and they can be generated only via indefinite recursions. The recursions are based on the so-called dilation equations, which express a wavelet or scaling function at a given resolution in terms of scaling functions of twice the resolution:

$$\phi(t) = 2^{1/2} \sum_{k=0}^{M-1} g_k \phi(2t - k), \qquad \psi(t) = 2^{1/2} \sum_{k=0}^{M-1} h_k \phi(2t - k).$$

These recursions are defined by the scaling-function coefficients g_k, which constitute a half-band lowpass filter, and by the wavelet coefficients h_k, which constitute a half-band highpass filter.

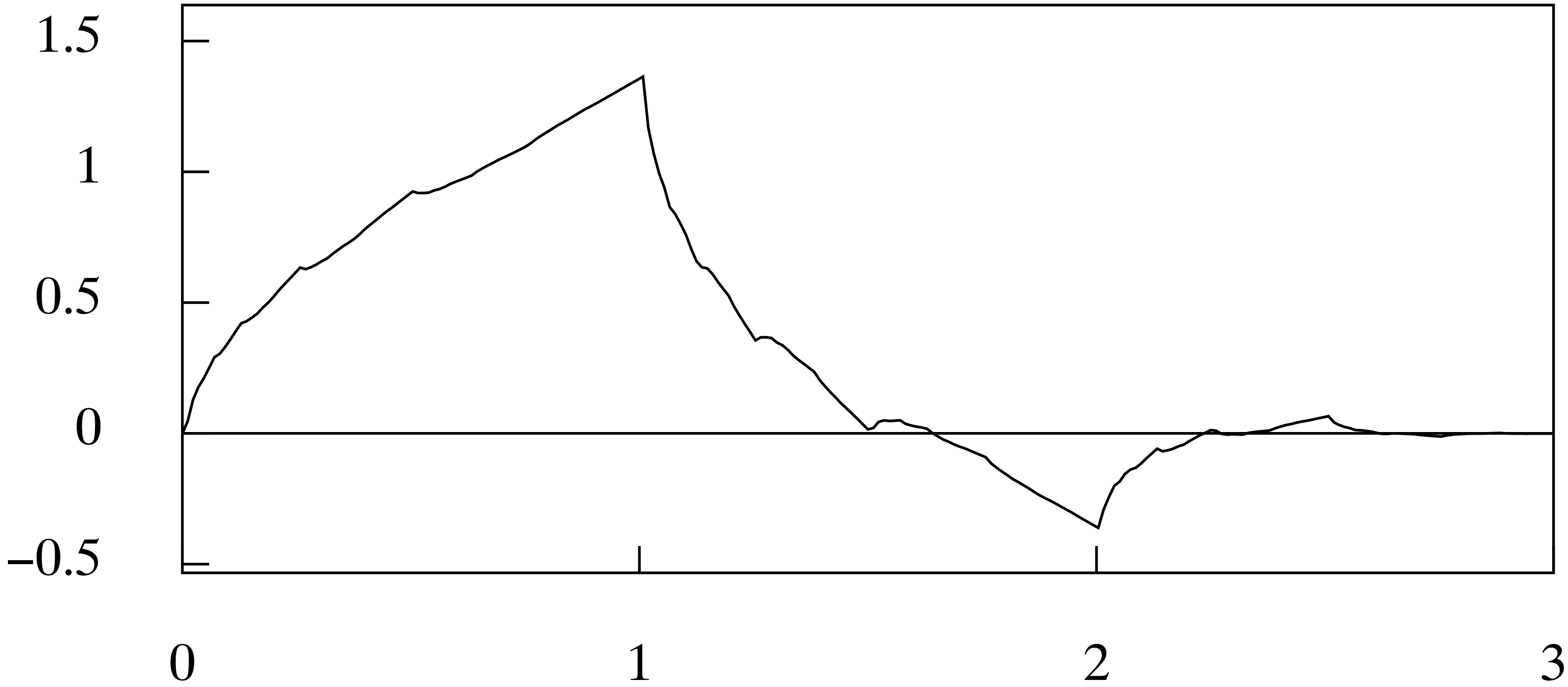

Figure 8. The Daubechies D4 scaling function calculated via a recursive method.

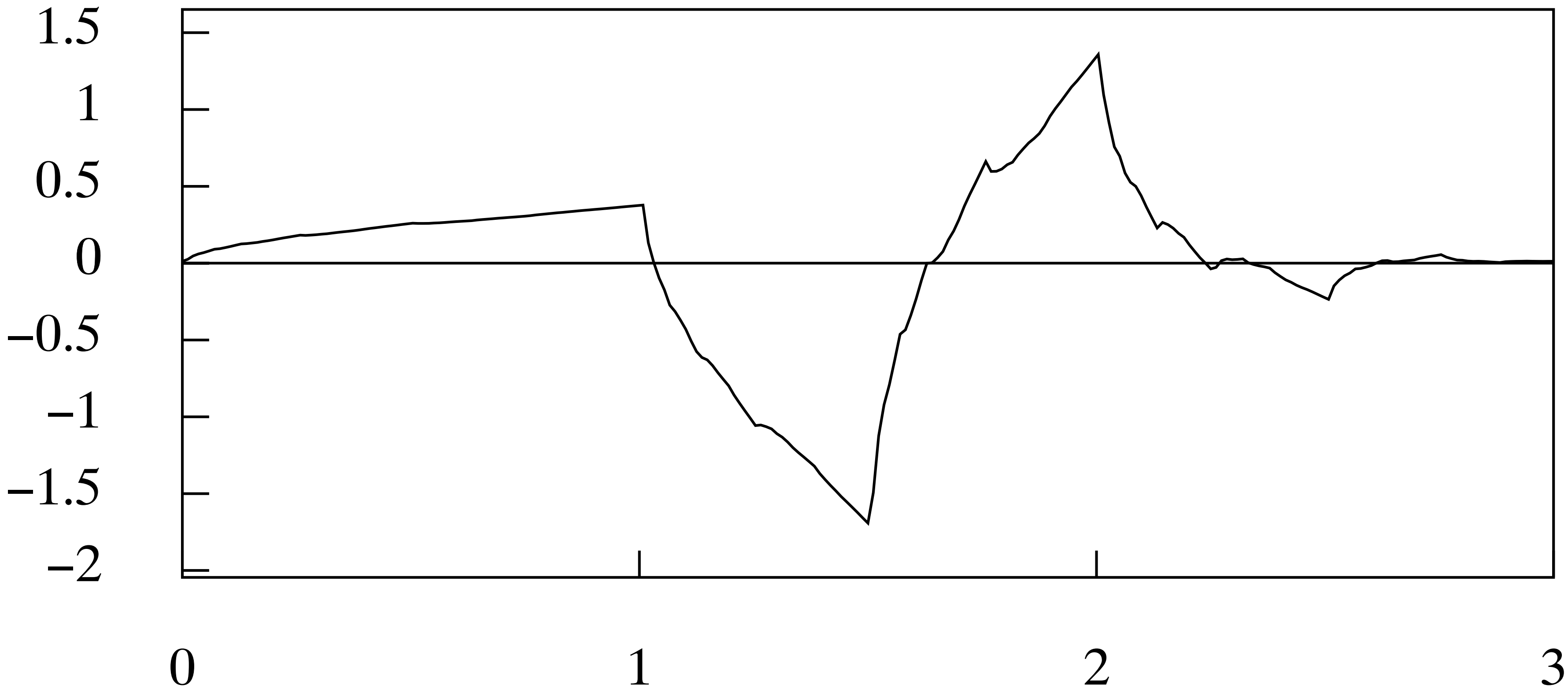

Figure 9. The Daubechies D4 wavelet function calculated via a recursive method.

Conditions of Orthogonality

The scaling functions displaced one from another by an even number $2m$ of points are *sequentially* orthogonal. The conditions of orthonormality are reflected in the filter coefficients. Thus

$$p_0 = \sum_{k=0}^{M-1} g_k^2 = 1 \quad \text{and} \quad p_{2m} = \sum_k g_k g_{k+2m} = 0.$$

The wavelet filter coefficient obey analogous conditions of orthogonality. The two sets of filter coefficients are mutually, i.e. *laterally,* orthogonal:

$$\sum_k g_k h_{k+2m} = 0.$$

This condition can be realised by setting

$$h_k = (-1)^k g_{M-1-k}, \quad \text{which implies that} \quad g_k = (-1)^{k+1} h_{M-1-k}.$$

An example is provided by the case where $M = 4$. Then, there are

$$\begin{aligned} &g_0, && h_0 = g_3, \\ &g_1, && h_1 = -g_2, \\ &g_2, && h_2 = g_1, \\ &g_3, && h_3 = -g_0. \end{aligned}$$

Complementary Filters: Sequential Orthogonality

The z-transforms of the lowpass and highpass filters in the case of a filter span of $M = 4$ are, respectively,

$$G(z) = g_0 + g_1 z + g_2 z^2 + g_3 z^3 \quad \text{and}$$

$$H(z) = g_3 - g_2 z + g_1 z^2 - g_0 z^3 = -z^3 G(-z^{-1}).$$

The corresponding autocovariance generating functions are $G(z)G(z^{-1}) = P(z)$ and $H(z)H(z^{-1}) = G(-z)G(-z^{-1}) = P(-z)$.

The condition of sequential orthogonality for the scaling function is equivalent to the condition that $P(z) + P(-z) = 2$, which gives

$$G(z)G(z^{-1}) + G(-z)G(-z^{-1}) = G(z)G(z^{-1}) + H(z)H(z^{-1}) = 2.$$

This amounts to the condition that $G(z)$ and $H(z)$ constitute complementary filters—the filter gain being 2 rather than unity.

Setting $z = \exp\{\mathrm{i}\omega\}$ with $\omega \in [-\pi, \pi]$ within $H(z)H(z^{-1})$ and $G(-z)G(-z^{-1})$ gives the squared gains of the filters.

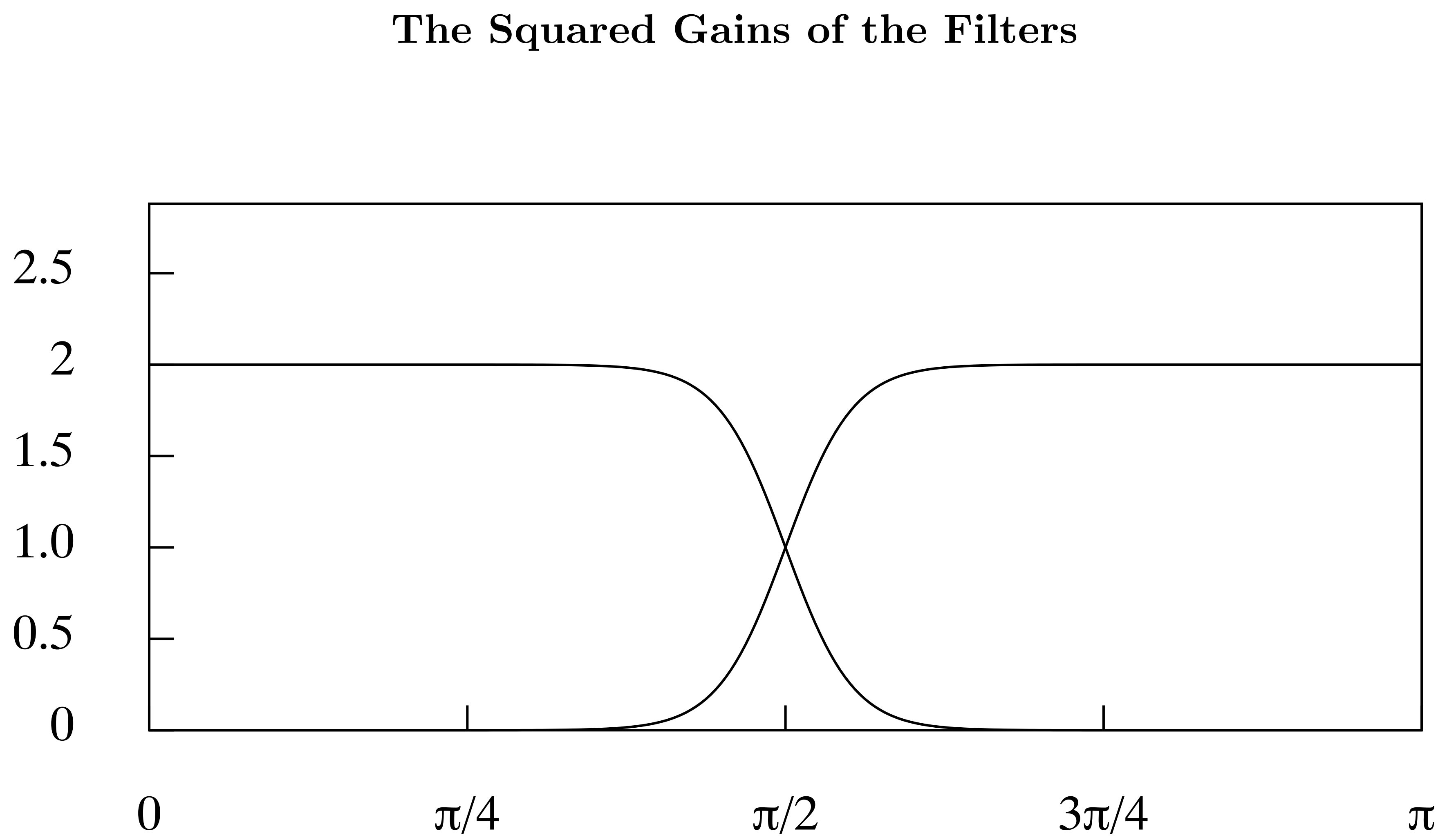

Figure 10. The squared gains of the complementary lowpass and highpass filters.

Complementary Filters: Lateral Orthogonality

The cross-covariance generating function formed from the coefficients of the highpass and lowpass filters is $G(z)H(z^{-1}) = Q(z)$.

The condition for lateral orthogonality is that

$$Q(z) + Q(-z) = G(z)H(z^{-1}) + G(-z)H(-z^{-1}) = 0.$$

Given that

$$G(-z) = g_0 - g_1 z + g_2 z^2 - g_3 z^3 = -z^3 H(z^{-1}) \quad \text{and}$$
$$H(-z^{-1}) = g_3 + g_2 z^{-1} + g_1 z^{-2} + g_0 z^{-3} = z^{-3} G(z),$$

it follows that the condition for lateral orthogonality is automatically satisfied by choosing $G(z)$ and $H(z)$ to be complementary filters.

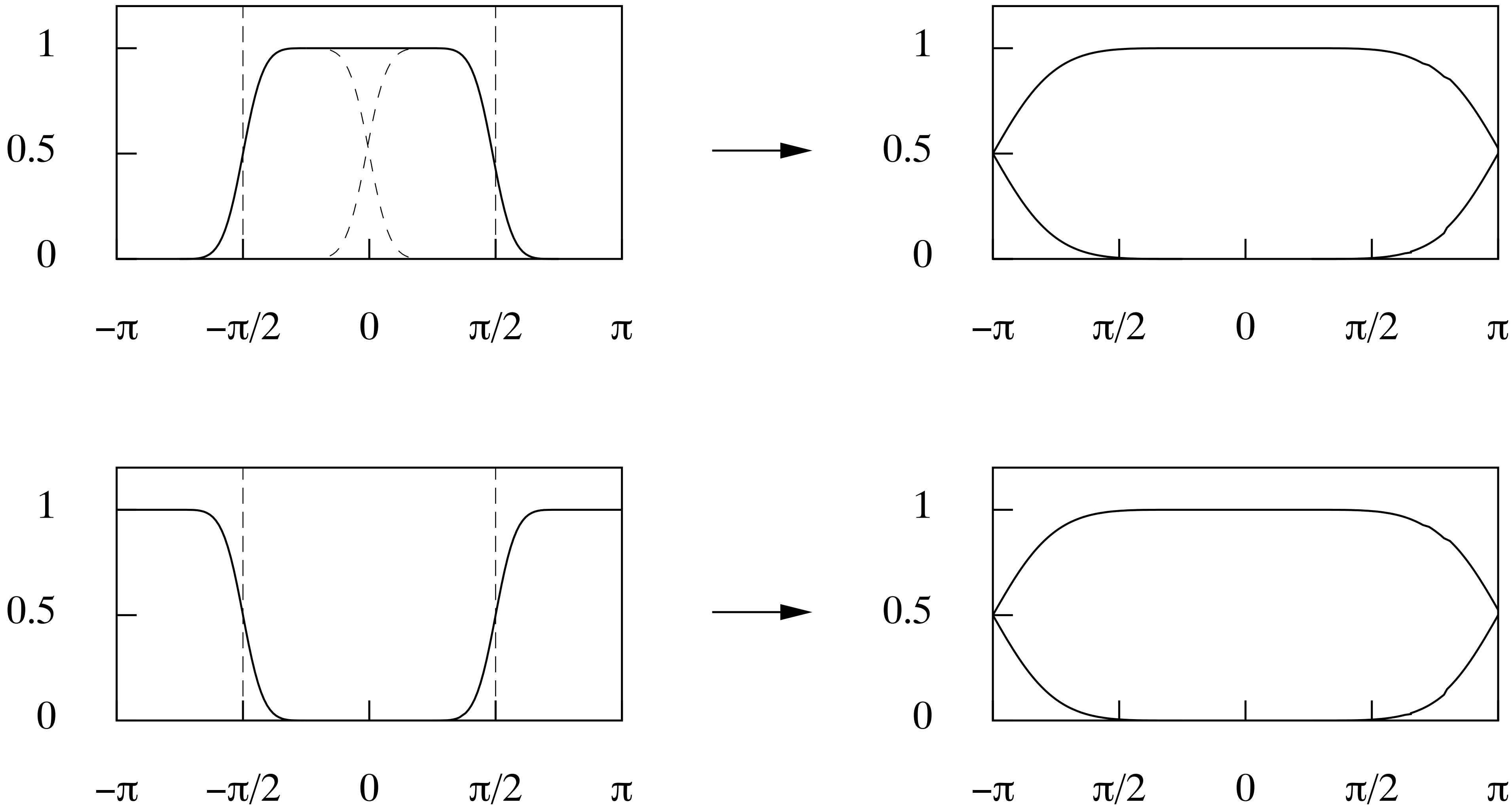

Figure 11. The consequence of dilating the gain functions of the complementary lowpass and highpass filters by a factor of 2 is to create an uniform spectral density function on the interval $[-\pi, \pi]$ of the kind that pertains to a white-noise process.

Spectral Dilation

The complementarity of the filters has an additional spectral implication relating to the sequential orthogonality of the wavelets/scaling functions and the corresponding filter coefficients at two-point displacements.

Let $P(t) \longleftrightarrow P(\omega)$ be the autocorrelation function and its Fourier transform. The condition that $P(2t) = 0$ for $t \in \{\pm 1, \pm 2, \ldots\}$, which is the condition of sequential orthogonality, is equivalent to the condition that $P(\omega/2) = 2$ when $\omega \in [0, \pi]$, which is that the frequency-domain function dilated by a factor of 2 has a uniform white-noise spectrum.

In fact, some account must also be taken of the negative frequency range. Thus, the true condition is that

$$P(\omega/2) + P(\pi + \omega/2) = 2 \quad \text{for} \quad \omega \in [-\pi, \pi].$$

The condition relies on the fact that the centres of $P(\omega)$ and $P(\pi + \omega)$ are separated by π radians. In other cases, such as that of the filter with a frequency bandwidth of $\pi/2$, running from $3\pi/8$ to $7\pi/8$, i.e. with a centre at $5/8\pi$, a dilation by a factor of 4 is required in order to achieve a uniform spectrum.

A Dyadic Wavelets Decomposition

There is liable to be a disparity between the frequency-limited nature of a signal $f(t)$ and the unbounded frequency content of wavelets on finite supports. A synthesis based on such wavelets is bound to be approximation:

$$f(t) \simeq \sum_{k=0}^{T-1} y_k \phi_0(t-k).$$

The T amplitude coefficients that are associated with the basis functions $\phi_0(t-k)$ are the sampled values.

The purpose of a wavelets analysis is to transform the T data values into a hierarchy of T coefficients that are associated with an alternative basis, which is ordered both according to the temporal locations of the wavelets and according to their frequency contents.

The hierarchy of wavelets is described by a so-called mosaic diagram that defines a partitioning of the time-frequency plane. This is illustrated for a sample of size $T = 128 = 2^7$. The height of a cell corresponds to a bandwidth in the frequency domain, whereas its width denotes a temporal duration.

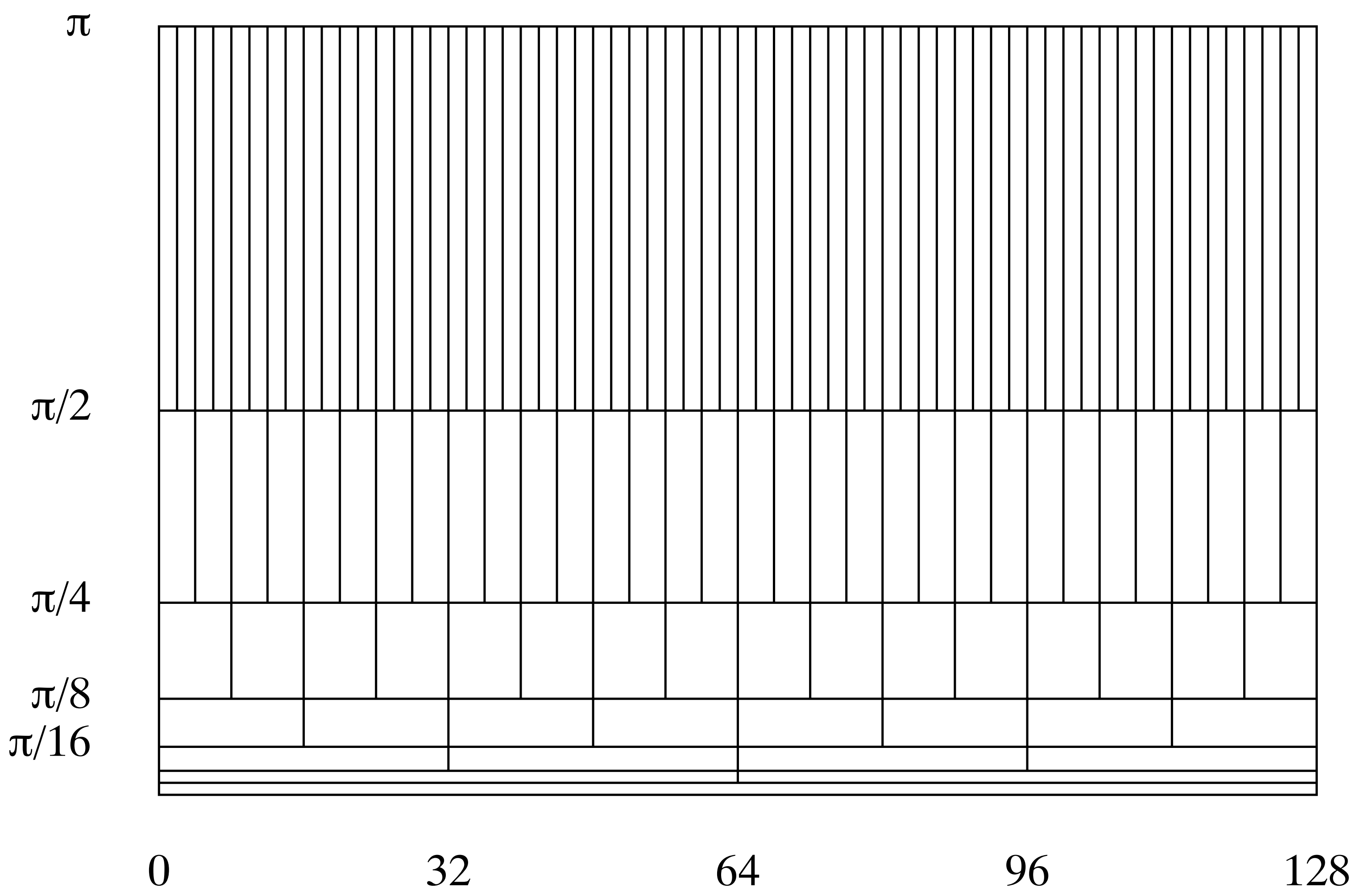

Figure 12. The partitioning of the time–frequency plane according to a multiresolution analysis of a data sequence of $128 = 2^7$ points.

The Pyramid Algorithm

The Pyramid Algorithm begins by filtering the data sequence of T points via a complementary pair of highpass and lowpass filters to generate two components of length T.

The components are downsampled by selecting alternate elements to give two sequences of length $T/2$. The downsampled high-frequency component contains the amplitude coefficients of the level-1 wavelets

The downsampled low-frequency component is subjected to a second round of filtering and sub sampling to generate high-frequency and low-frequency sequences of length $T/4$.

The downsampled high-frequency component contains the amplitude coefficients of the level-2 wavelets. The downsampled low-frequency component becomes the subject of the next round of filtering.

The process continues until it exhausts the available data. The effect is to convert the data into set to T amplitude coefficients that can be associated with the hierarchy of wavelets and with the final scaling function or functions.

A Regression Analogy

A discrete dyadic wavelets analysis entails an orthonormal matrix transform Q that delivers a vector $\beta = Q'y$ of wavelet amplitude coefficients. The data can be synthesised via the inverse transform $y = Q'\beta = QQ'y$. A frequency-specific component of the data is $y_j = Q_jQ_j'y$, where Q_j contains columns of Q.

For an analogy, consider an ordinary normal regression model $N(y, X\beta, \sigma^2 I)$ estimated by OLS. There is

$$y - X\beta = \varepsilon = P\varepsilon + (I - P)\varepsilon \quad \text{with} \quad P = X(X'X)^{-1}X'.$$

Define a partitioned orthonormal matrix $C = [C_1, C_2]$ such that $P = C_1C_1'$ and $(I - P) = C_1C_1'$. Then, there are $\eta_1 = C_1'\varepsilon \sim N(0, \sigma^2 I_k)$ and $\eta_2 = C_2'\varepsilon \sim N(0, \sigma^2 I_{T-K})$, and we may form

$$\frac{\varepsilon' C_1 C_1' \varepsilon}{\sigma^2} = \frac{\eta_1\eta_1'}{\sigma^2} = \frac{(\beta - b)'X'X(\beta - b)}{\sigma^2} \sim \chi^2(k) \quad \text{and}$$
$$\frac{\varepsilon' C_2 C_2' \varepsilon}{\sigma^2} = \frac{\eta_2\eta_2'}{\sigma^2} = \frac{(y - Xb)'(y - Xb)}{\sigma^2} = \frac{e'e}{\sigma^2} \sim \chi^2(T - k).$$

The vector $\eta = [\eta_1', \eta_2']'$ is analogous to the vector β of wavelets amplitude coefficients.

Circulant Matrices

The circulant matrix that is the analogue of the matrix lag operator is $K_T = [e_1, e_2, \ldots, e_{T-1}, e_0]$. This is obtained from the matrix $I_T = [e_0, e_1, \ldots, e_{T-1}]$ by displacing the leading column to the end of the array.

An example is provided by K_4 and its powers:

$$K_4 = \begin{bmatrix} 0 & 0 & 0 & 1 \\ 1 & 0 & 0 & 0 \\ 0 & 1 & 0 & 0 \\ 0 & 0 & 1 & 0 \end{bmatrix}, \quad K_4^2 = \begin{bmatrix} 0 & 0 & 1 & 0 \\ 0 & 0 & 0 & 1 \\ 1 & 0 & 0 & 0 \\ 0 & 1 & 0 & 0 \end{bmatrix}, \quad K_4^3 = \begin{bmatrix} 0 & 1 & 0 & 0 \\ 0 & 0 & 1 & 0 \\ 0 & 0 & 0 & 1 \\ 1 & 0 & 0 & 0 \end{bmatrix}.$$

The matrices $K_T^0 = I_T, K_T, \ldots, K_T^{T-1}$ form a basis for the set of all circulant matrices of order T

There is a one-to-one correspondence between the set of all polynomials of degree less than T and the set of all circulant matrices of order T. If $\alpha(z)$ is a polynomial of degree less that T, then the corresponding circulant matrix is

$$A = \alpha(K_T) = \alpha_0 I_T + \alpha_1 K_T + \cdots + \alpha_{T-1} K_T^{T-1}.$$

Upsampling and Downsampling Matrices

The downsampling matrix V removes alternate elements from a vector, beginning with second element. The upsampling matrix $\Lambda = \mathrm{V}'$ interpolates zeros between the elements of a vector. These matrices are exemplified by

$$
\mathrm{V} = \begin{bmatrix} 1 & 0 & 0 & 0 & 0 & 0 & 0 & 0 \\ 0 & 0 & 1 & 0 & 0 & 0 & 0 & 0 \\ 0 & 0 & 0 & 0 & 1 & 0 & 0 & 0 \\ 0 & 0 & 0 & 0 & 0 & 0 & 1 & 0 \end{bmatrix} \qquad \text{and} \qquad \Lambda = \begin{bmatrix} 1 & 0 & 0 & 0 \\ 0 & 0 & 0 & 0 \\ 0 & 1 & 0 & 0 \\ 0 & 0 & 0 & 0 \\ 0 & 0 & 1 & 0 \\ 0 & 0 & 0 & 0 \\ 0 & 0 & 0 & 1 \\ 0 & 0 & 0 & 0 \end{bmatrix}.
$$

Downsampling and Mirror Image Reversals

The spectrum or the periodogram of a real-valued data sequence is a symmetric function of the frequency interval $[-\pi, \pi]$. The portions on the subintervals $[-\pi, 0]$ and $[0, \pi]$ being mirror images.

Downsampling alters the frequency content of a temporal sequence. A low-frequency content that is confined to the interval $[-\pi/2, \pi/2]$ will be mapped onto the full Nyquist interval $[-\pi, \pi]$.

The portions on the intervals $[-\pi, 0]$ and $[0, \pi]$ are dilated versions of what was previously on the intervals $[-\pi/2, 0]$ and $[0, \pi/2]$ respectively.

A high-frequency content that is confined to $[-\pi, -\pi/2] \cup [\pi, \pi/2]$ will also be mapped onto the interval $[-\pi, \pi]$.

The portion previously on the interval $[-\pi, -\pi/2]$ will be found in dilated form of the interval $[0, \pi]$ and the portion previously on the interval $[\pi/2, \pi]$ will be found, in dilated form, of the interval $[-\pi, 0]$.

Thus, the high frequency content of $[0, \pi]$ will be replaced by a dilated version of its mirror image. A *lowpass filter* will be required in order to isolate its *high-frequency* content.

The Effects of Downsampling on the Periodogram

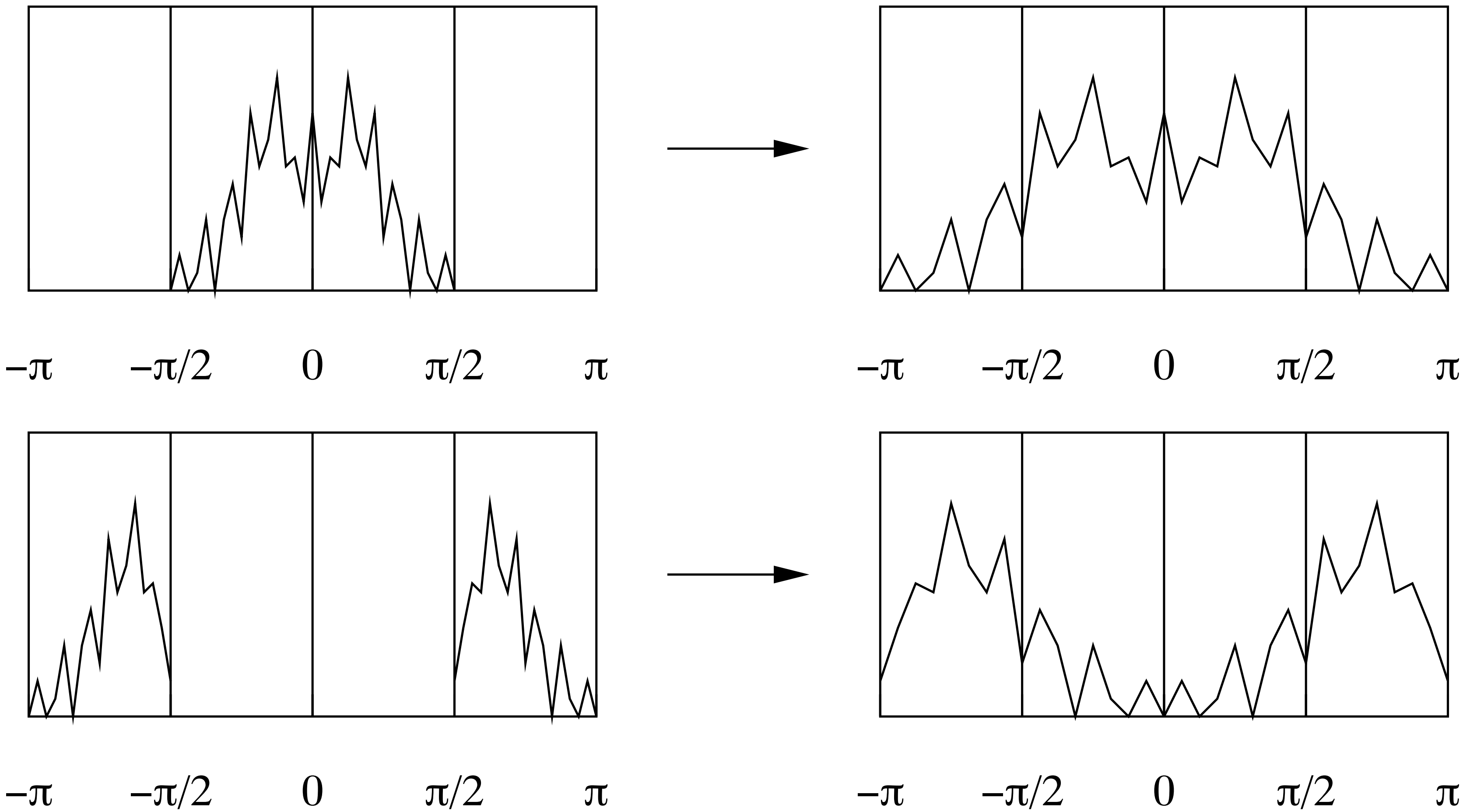

Figure 13. In the process of downsampling, the high frequency content of $[0, \pi]$ will be replaced by a dilated version of its mirror image.

A Circulant Filter Matrix

The highpass filter that is to be applied to the data in the first round of the wavelets decomposition has the following matrix representation:

$$H_{(1)} = \begin{bmatrix} h_0 & 0 & 0 & 0 & 0 & h_3 & h_2 & h_1 \\ h_1 & h_0 & 0 & 0 & 0 & 0 & h_3 & h_2 \\ h_2 & h_1 & h_0 & 0 & 0 & 0 & 0 & h_3 \\ h_3 & h_2 & h_1 & h_0 & 0 & 0 & 0 & 0 \\ 0 & h_3 & h_2 & h_1 & h_0 & 0 & 0 & 0 \\ 0 & 0 & h_3 & h_2 & h_1 & h_0 & 0 & 0 \\ 0 & 0 & 0 & h_3 & h_2 & h_1 & h_0 & 0 \\ 0 & 0 & 0 & 0 & h_3 & h_2 & h_1 & h_0 \end{bmatrix}.$$

Premultiplying this by the down sampling matrix is a matter of deleting alternate rows:

$$\mathrm{V}H_{(1)} = \begin{bmatrix} h_0 & 0 & 0 & 0 & 0 & h_3 & h_2 & h_1 \\ h_2 & h_1 & h_0 & 0 & 0 & 0 & 0 & h_3 \\ 0 & h_3 & h_2 & h_1 & h_0 & 0 & 0 & 0 \\ 0 & 0 & 0 & h_3 & h_2 & h_1 & h_0 & 0 \end{bmatrix}.$$

The First Round of the Pyramid Algorithm

When this matrix is combined with the matrix $\mathrm{V}G_{(1)}$, which is the down sampled version of the lowpass filter matrix, and when the data vector y is mapped through the combined matrix, the result is

$$\begin{bmatrix} \beta_{10} \\ \beta_{11} \\ \beta_{12} \\ \beta_{13} \\ \hline \gamma_{10} \\ \gamma_{11} \\ \gamma_{12} \\ \gamma_{13} \end{bmatrix} = \begin{bmatrix} h_0 & 0 & 0 & 0 & 0 & h_3 & h_2 & h_1 \\ h_2 & h_1 & h_0 & 0 & 0 & 0 & 0 & h_3 \\ 0 & h_3 & h_2 & h_1 & h_0 & 0 & 0 & 0 \\ 0 & 0 & 0 & h_3 & h_2 & h_1 & h_0 & 0 \\ \hline g_0 & 0 & 0 & 0 & 0 & g_3 & g_2 & g_1 \\ g_2 & g_1 & g_0 & 0 & 0 & 0 & 0 & g_3 \\ 0 & g_3 & g_2 & g_1 & g_0 & 0 & 0 & 0 \\ 0 & 0 & 0 & g_3 & g_2 & g_1 & g_0 & 0 \end{bmatrix} \begin{bmatrix} y_0 \\ y_1 \\ y_2 \\ y_3 \\ y_4 \\ y_5 \\ y_6 \\ y_7 \end{bmatrix}.$$

The transformation can be represented, in summary notation, by

$$\begin{bmatrix} \beta_{(1)} \\ \gamma_{(1)} \end{bmatrix} = \begin{bmatrix} \mathrm{V}H_{(1)} \\ \mathrm{V}G_{(1)} \end{bmatrix} y.$$

The Second Round of the Pyramid Algorithm

In the second round of the wavelets decomposition, the coefficients associated with the level-1 wavelets are preserved and the coefficients associated with the level-1 scaling functions are subject to a further decomposition:

$$\begin{bmatrix} \beta_{10} \\ \beta_{11} \\ \beta_{12} \\ \beta_{13} \\ \hline \beta_{20} \\ \beta_{21} \\ \hline \gamma_{20} \\ \gamma_{21} \end{bmatrix} = \left[\begin{array}{cccc|cccc} 1 & 0 & 0 & 0 & 0 & 0 & 0 & 0 \\ 0 & 1 & 0 & 0 & 0 & 0 & 0 & 0 \\ 0 & 0 & 1 & 0 & 0 & 0 & 0 & 0 \\ 0 & 0 & 0 & 1 & 0 & 0 & 0 & 0 \\ \hline 0 & 0 & 0 & 0 & h_0 & h_3 & h_2 & h_1 \\ 0 & 0 & 0 & 0 & h_2 & h_1 & h_0 & h_3 \\ \hline 0 & 0 & 0 & 0 & g_0 & g_3 & g_2 & g_1 \\ 0 & 0 & 0 & 0 & g_2 & g_1 & g_0 & g_3 \end{array}\right] \begin{bmatrix} \beta_{10} \\ \beta_{11} \\ \beta_{12} \\ \beta_{13} \\ \hline \gamma_{10} \\ \gamma_{11} \\ \gamma_{12} \\ \gamma_{13} \end{bmatrix}.$$

The summary notation for this is

$$\begin{bmatrix} \beta_{(1)} \\ \beta_{(2)} \\ \gamma_{(2)} \end{bmatrix} = \begin{bmatrix} I & 0 \\ 0 & \mathrm{V}H_{(2)} \\ 0 & \mathrm{V}G_{(2)} \end{bmatrix} \begin{bmatrix} \beta_{(1)} \\ \gamma_{(1)} \end{bmatrix}.$$

The Completed Analysis

The third and final transformation can represented equally by

$$\begin{bmatrix} \gamma_{30} \\ \beta_{30} \end{bmatrix} = \begin{bmatrix} h_0 & h_3 & h_2 & h_1 \\ g_0 & g_3 & g_2 & g_1 \end{bmatrix} \begin{bmatrix} \gamma_{20} \\ \gamma_{21} \\ \gamma_{20} \\ \gamma_{21} \end{bmatrix}$$

or by

$$\begin{bmatrix} \gamma_{30} \\ \beta_{30} \end{bmatrix} = \begin{bmatrix} h_0 + h_2 & h_3 + h_1 \\ g_0 + g_2 & g_3 + g_1 \end{bmatrix} \begin{bmatrix} \gamma_{20} \\ \gamma_{21} \end{bmatrix}.$$

The vector of amplitude coefficients associated with the wavelet on the jth level is

$$\beta_{(j)} = \mathrm{V}H_{(j)}\mathrm{V}G_{(j-1)} \cdots \mathrm{V}G_{(1)}y = Q'_{(j)}y.$$

Here, $Q'_{(j)}$is formed from a set of adjacent rows of Q'.

The component vector $w_j = [w_{0j}, w_{1j}, \ldots, w_{T-1,j}]'$ of the decomposition of $y = w_1 + \cdots + w_n + v_n$ is synthesised as follows:

$$w_j = Q_{(j)}\beta_{(j)} = G'_{(1)}\Lambda \cdots G'_{(j-1)}\Lambda H'_{(j)}\Lambda\beta_{(j)}.$$

The Flow Diagram of the Analysis Section

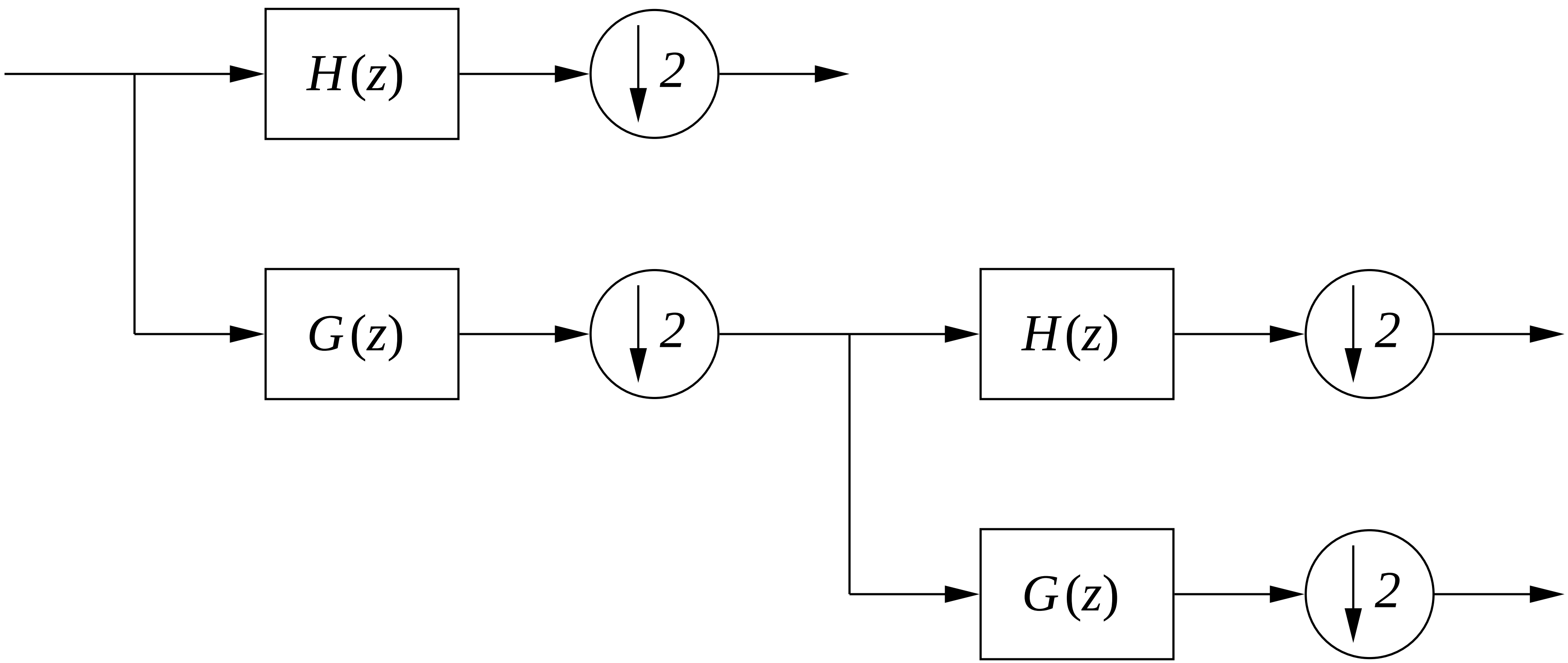

Figure 14. The analysis section of a dyadic filter bank, expressed in terms of z-transform polynomials.

The Flow Diagram of the Synthesis Section

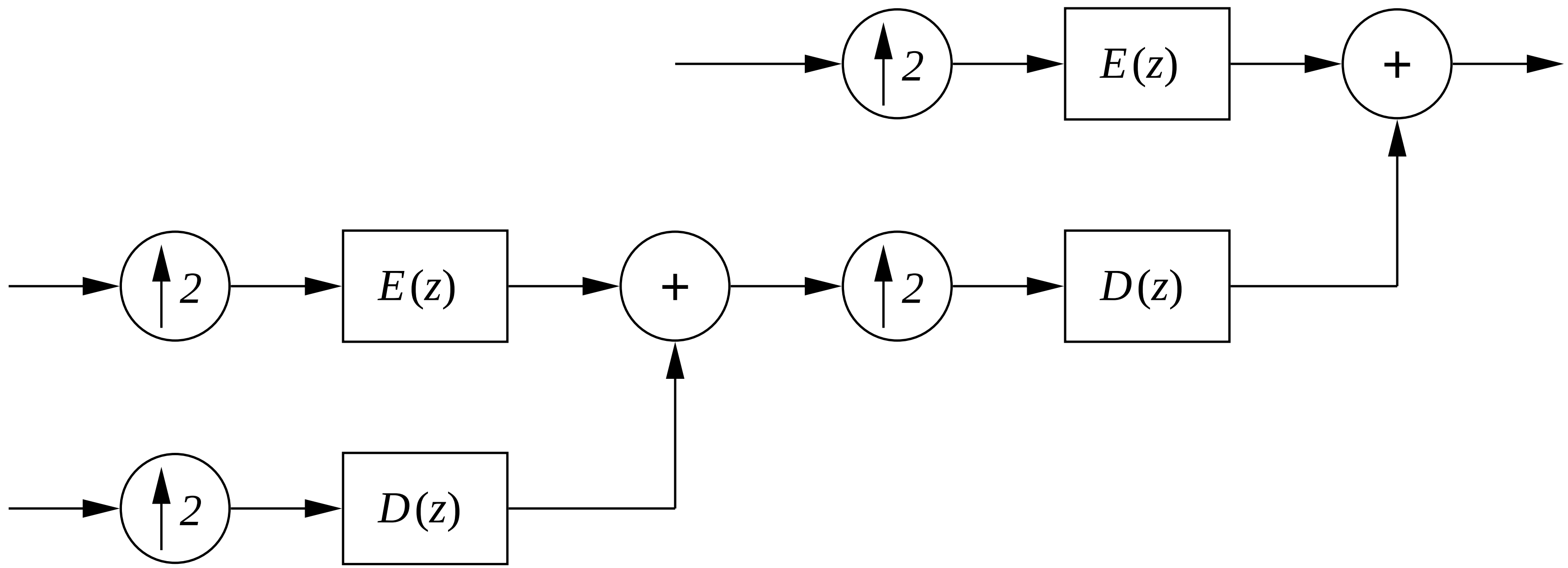

Figure 15. The synthesis section of a dyadic filter bank, expressed in terms of z-transform polynomials.

The Flow Diagram of the Two-Channel Filter Bank

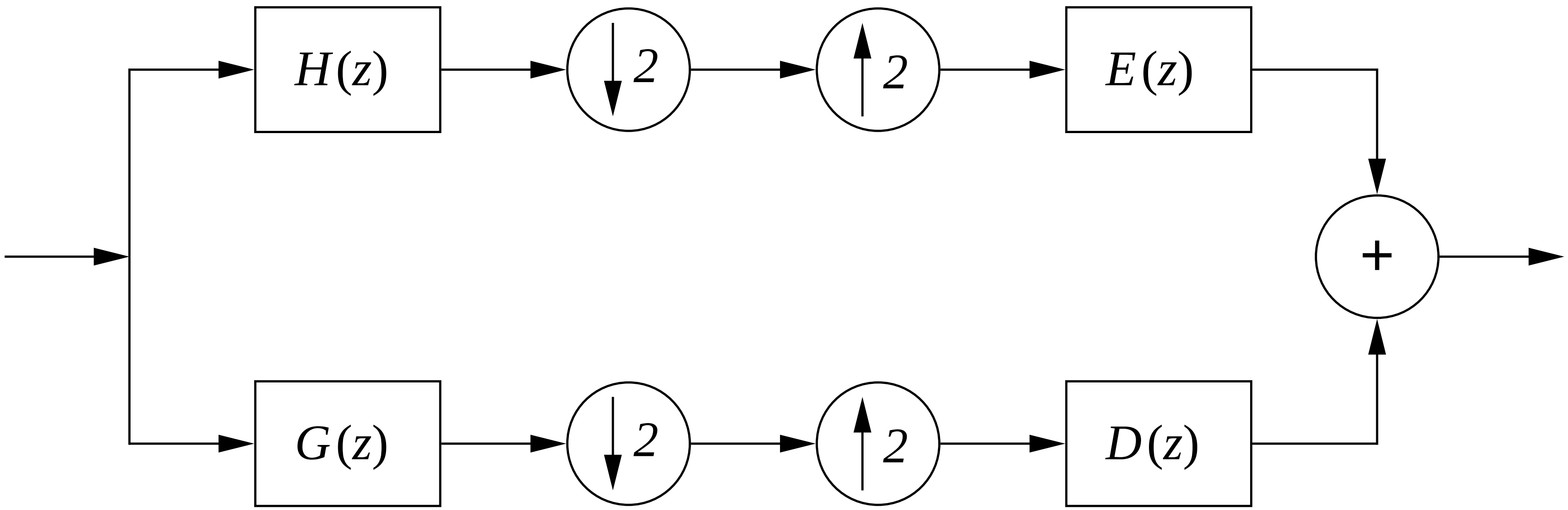

Figure 16. In the two-channel filter bank, perfect reconstruction can be achieved by setting $E(z) = H(z^{-1})$ and $D(z) = G(z^{-1})$.

Perfect Reconstruction

The signals that emerge from the two branches of the filter bank are

$$w(z) = \frac{1}{2}E(z)\{H(z)x(z) + H(-z)x(-z)\} \quad \text{and,}$$

$$v(z) = \frac{1}{2}D(z)\{G(z)x(z) + G(-z)x(-z)\}.$$

Combining them gives

$$\begin{aligned} y(z) = \frac{1}{2}&\{D(z)G(-z) + E(z)H(-z)\}x(-z), \\ &+ \frac{1}{2}\{D(z)G(z) + E(z)H(z)\}x(z). \end{aligned}$$

The term in $x(-z)$ is due to aliasing; and it can be eliminated by setting

$$D(z) = z^{-(M-1)}H(-z) = G(z^{-1}), \qquad E(z) = -z^{-(M-1)}G(-z) = H(z^{-1}).$$

In that case, $y(z) = x(z)$, and there is perfect reconstruction.

A Dyadic Wavelet Packet Analysis

In a regular dyadic wavelets packet analysis, the bands that partition the frequency interval $[0, \pi]$ are of equal width. Their number is constrained to be of the form $q = T/2^m$, where $T = 2^n$ is the sample size.

The bands are obtained by successive divisions of both the highpass and the lowpass outputs of the two-channel filter bank.

The mirror-image reversals that affect the output of the highpass band after downsampling implies that, in the second round of filtering, its lowpass content will be extracted by the filter $H(z)$, which is nominally a highpass filter, and that its highpass content will be extracted by $G(z)$, which is nominally a lowpass filter.

The effect of the mirror-image reversals in subsequent rounds of filtering can be illustrated via the relevant mosaic diagram.

Adjacent bands of equal width that are produced by a regular decomposition can be combined. This is achieved by halting the process of subdivision within selected channels.

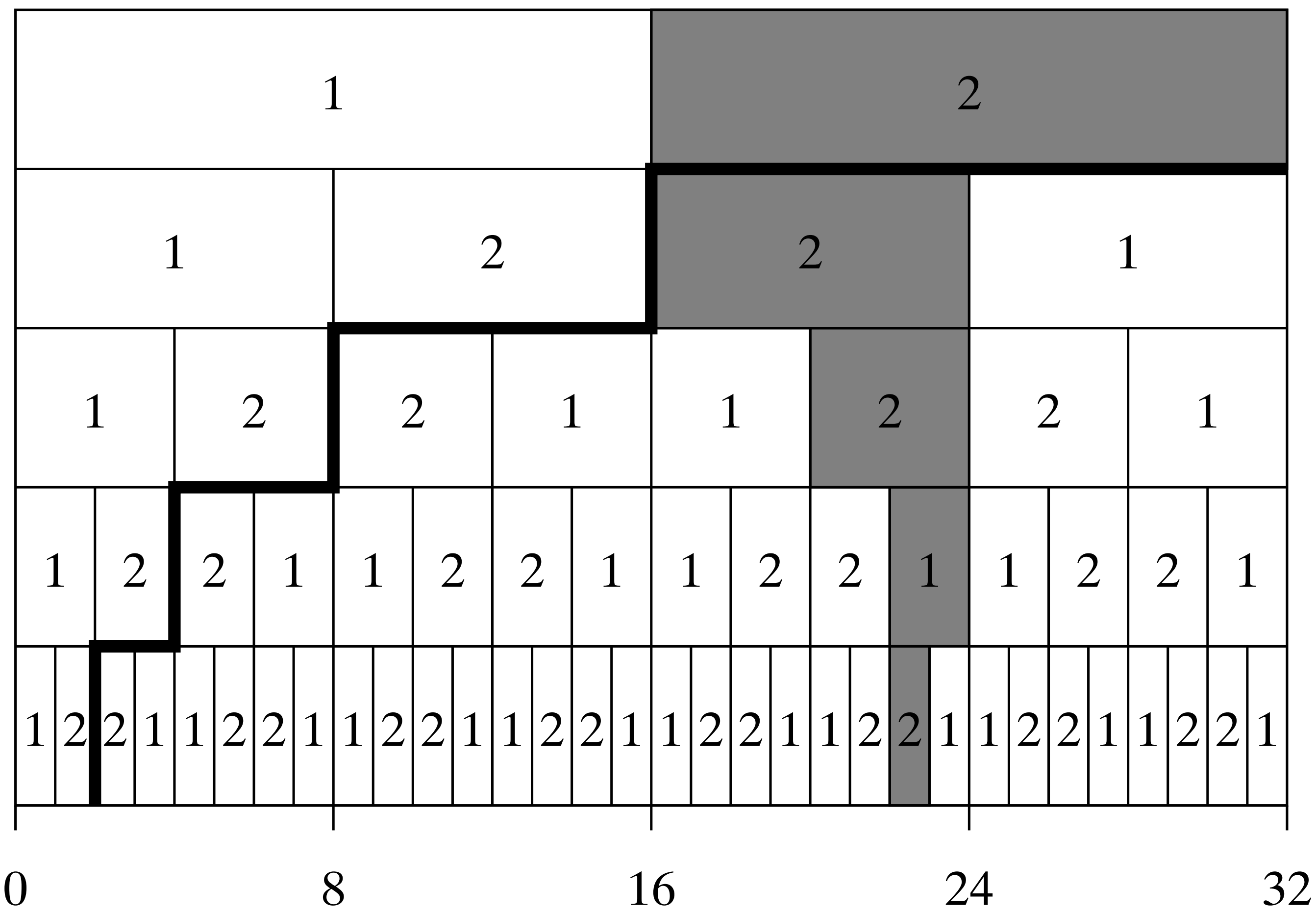

Figure 17. The scheme for constructing compound filters in the dyadic case. The diagram highlights the construction of the filter $\psi_{23/32}(\omega)$. The bold line demarcates an ordinary dyadic octave analysis.

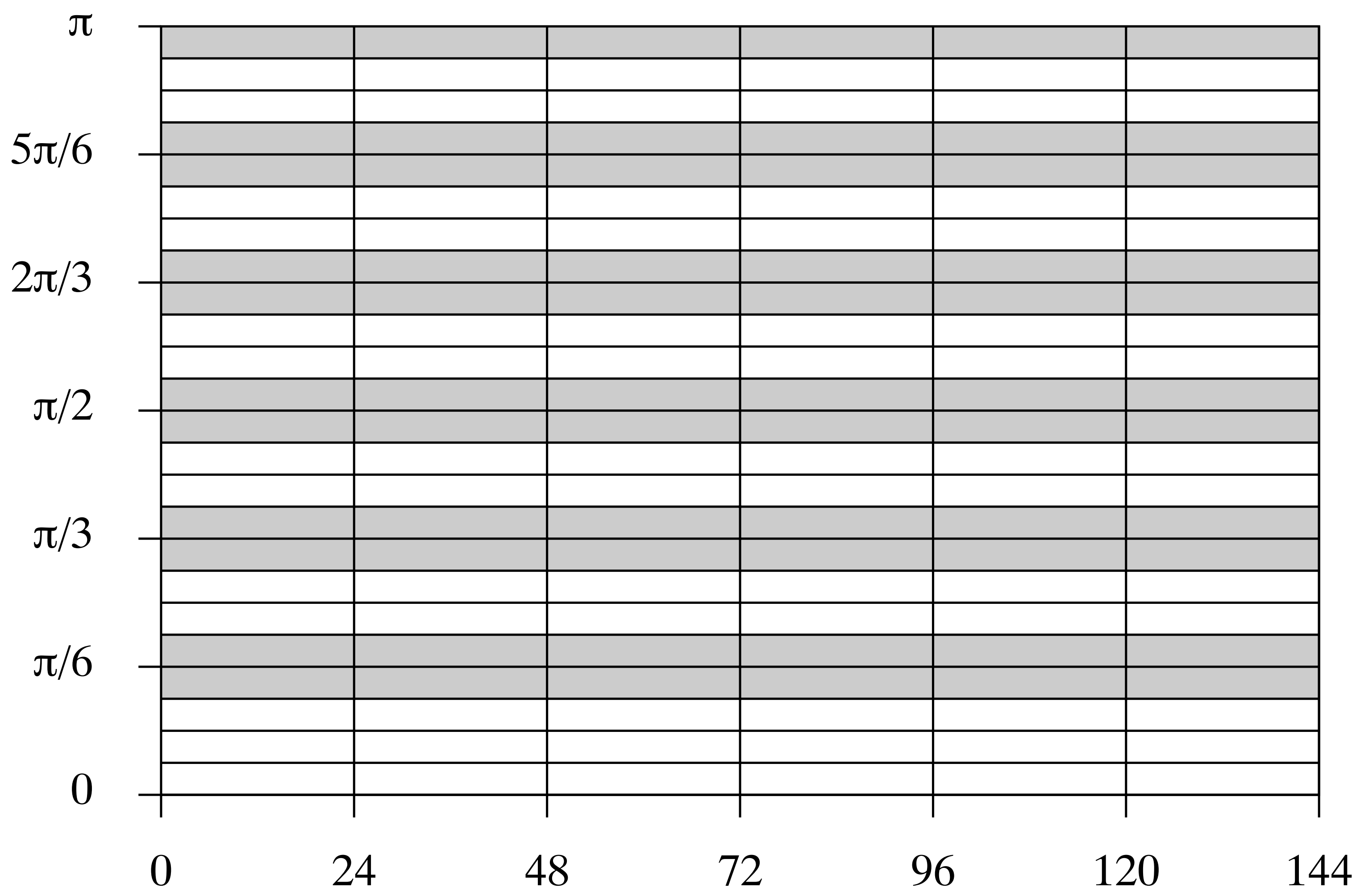

Figure 18. The time–frequency plane for $144 = 3^2 \times 2^4$ data points partitioned with 24 frequency intervals and 6 time periods. The non-dyadic mosaic is relevant to the analysis of the seasonal fluctutions of the airline passenger data.

A Two-Phase Two-Channel Architecture

Consider a two-channel architecture that separates the odd and even phases of the data vector:

$$\begin{bmatrix} \beta_{10} \\ \beta_{11} \\ \beta_{12} \\ \beta_{13} \\ \hline \gamma_{10} \\ \gamma_{11} \\ \gamma_{12} \\ \gamma_{13} \end{bmatrix} = \begin{bmatrix} h_0 & 0 & 0 & h_2 \\ h_2 & h_0 & 0 & 0 \\ 0 & h_2 & h_0 & 0 \\ 0 & 0 & h_2 & h_0 \\ \hline g_0 & 0 & 0 & g_2 \\ g_2 & g_0 & 0 & 0 \\ 0 & g_2 & g_0 & 0 \\ 0 & 0 & g_2 & g_0 \end{bmatrix} \begin{bmatrix} y_0 \\ y_2 \\ y_4 \\ y_6 \end{bmatrix} + \begin{bmatrix} 0 & 0 & h_3 & h_1 \\ h_1 & 0 & 0 & h_3 \\ h_3 & h_1 & 0 & 0 \\ 0 & h_3 & h_1 & 0 \\ \hline 0 & 0 & g_3 & g_1 \\ g_1 & 0 & 0 & g_3 \\ g_3 & g_1 & 0 & 0 \\ 0 & g_3 & g_1 & 0 \end{bmatrix} \begin{bmatrix} y_1 \\ y_3 \\ y_5 \\ y_7 \end{bmatrix}.$$

This can be represented, in summary notation, by

$$\begin{bmatrix} \beta \\ \gamma \end{bmatrix} = \begin{bmatrix} H^e \\ G^e \end{bmatrix} y^e + \begin{bmatrix} KH^o \\ KG^o \end{bmatrix} y^o,$$

where $y^e = [y_0, y_2, y_4, y_6]' = \mathrm{V}y$ and $y^o = [y_1, y_3, y_5, y_7]' = \mathrm{V}Ky$. Also,

$$G^e = g_0 I_{T/2} + g_2 K_{T/2} \quad \text{and} \quad G^o = g_1 I_{T/2} + g_3 K_{T/2}.$$

The synthesis section can also be reformulated as follows:

$$
\begin{bmatrix} y_0 \\ y_2 \\ y_4 \\ y_6 \\ \hline y_1 \\ y_3 \\ y_5 \\ y_7 \end{bmatrix} = \begin{bmatrix} h_0 & h_2 & 0 & 0 \\ 0 & h_0 & h_2 & 0 \\ 0 & 0 & h_0 & h_2 \\ h_2 & 0 & 0 & h_0 \\ \hline 0 & h_1 & h_3 & 0 \\ 0 & 0 & h_1 & h_3 \\ h_3 & 0 & 0 & h_1 \\ h_1 & h_3 & 0 & 0 \end{bmatrix} \begin{bmatrix} \beta_0 \\ \beta_1 \\ \beta_2 \\ \beta_3 \end{bmatrix} + \begin{bmatrix} g_0 & g_2 & 0 & 0 \\ 0 & g_0 & g_2 & 0 \\ 0 & 0 & g_0 & g_2 \\ g_2 & 0 & 0 & g_0 \\ \hline 0 & g_1 & g_3 & 0 \\ 0 & 0 & g_1 & g_3 \\ g_3 & 0 & 0 & g_1 \\ g_1 & g_3 & 0 & 0 \end{bmatrix} \begin{bmatrix} \gamma_0 \\ \gamma_1 \\ \gamma_2 \\ \gamma_3 \end{bmatrix}.
$$

In summary notation, this becomes

$$
\begin{bmatrix} y^e \\ y^o \end{bmatrix} = \begin{bmatrix} H^{e\prime} \\ H^{o\prime}K' \end{bmatrix} \beta + \begin{bmatrix} G^{o\prime} \\ G^{o\prime}K' \end{bmatrix} \gamma.
$$

Perfect reconstruction is achieved, since the orthogonality conditions imply that

$$
\begin{bmatrix} H^{e\prime} & G^{o\prime} \\ H^{o\prime}K' & G^{o\prime}K' \end{bmatrix} \begin{bmatrix} H^e & KH^o \\ G^e & KG^o \end{bmatrix} = 2 \begin{bmatrix} I & 0 \\ 0 & I \end{bmatrix}.
$$

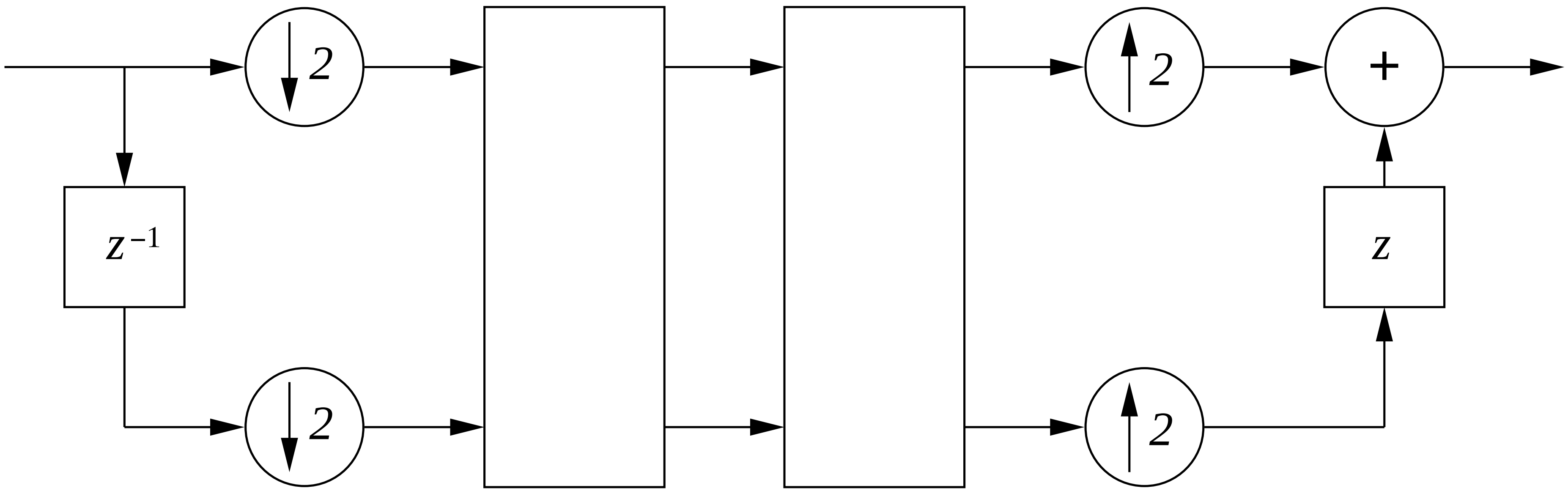

Figure 19. An alternative architecture for the two-channel filter bank separates the data points bearing even indices from those bearing odd indices.

A Triadic Multiphase Analysis

Consider a highpass filter $f(z)$ of six coefficients of which the nominal passband is the interval $[2\pi/3, \pi]$. Then,

$$\begin{aligned}
F(z) &= f_0 + f_1 z + \cdots + f_5 z^5 \\
&= (f_0 + f_3 z^3) + z(f_1 + f_4 z^3) + z^2(f_2 + f_5 z^3) \\
&= F_0(z) + zF_1(z) + z^2 F_2(z).
\end{aligned}$$

From the data sequence $y(t) = \{y_0, y_1, y_2, \cdots\}$ are derived the following three subsampled data sequences:

$$\begin{aligned}
y_0(t) &= \{y_0, y_3, y_6, \cdots\}, \\
y_1(t) &= \{y_1, y_4, y_7, \cdots\}, \\
y_2(t) &= \{y_3, y_5, y_8, \cdots\},
\end{aligned}$$

together with their z-transforms $y(z)$, $y_0(z)$,$y_1(z)$, and $y_2(z)$. Then,

$$F(z)y(z) = F_0(z)y_0(z) + zF_1(z)y_1(z) + z^2 F_2(z)y_2(z).$$

The RHS can be rendered in matrix notation as follows

$$\begin{bmatrix} f_0 & 0 & 0 & f_3 \\ f_3 & f_0 & 0 & 0 \\ 0 & f_3 & f_0 & 0 \\ 0 & 0 & f_3 & f_0 \end{bmatrix} \begin{bmatrix} y_0 \\ y_3 \\ y_6 \\ y_9 \end{bmatrix} + \begin{bmatrix} 0 & 0 & f_4 & f_1 \\ f_1 & 0 & 0 & f_4 \\ f_4 & f_1 & 0 & 0 \\ 0 & f_4 & f_1 & 0 \end{bmatrix} \begin{bmatrix} y_1 \\ y_4 \\ y_7 \\ y_{10} \end{bmatrix} + \begin{bmatrix} 0 & f_5 & f_2 & 0 \\ 0 & 0 & f_5 & f_2 \\ f_2 & 0 & 0 & f_5 \\ f_5 & f_2 & 0 & 0 \end{bmatrix} \begin{bmatrix} y_2 \\ y_5 \\ y_8 \\ y_{11} \end{bmatrix}$$

In summary notation, this is $\delta = F_0 y_0 + KF_1 y_1 + K^2 F_2 y_2$. There are three such transformations:

$$\begin{bmatrix} \beta \\ \gamma \\ \delta \end{bmatrix} = \begin{bmatrix} H_0 & KH_1 & K^2 H_2 \\ G_0 & KG_1 & K^2 G_2 \\ F_0 & KF_1 & K^2 F_2 \end{bmatrix} \begin{bmatrix} y_0 \\ y_1 \\ y_2 \end{bmatrix}.$$

The synthesis stage entails the inverse mapping

$$\begin{bmatrix} y_0 \\ y_1 \\ y_2 \end{bmatrix} \begin{bmatrix} H_0 & KH_1 & K^2 H_2 \\ G_0 & KG_1 & K^2 G_2 \\ F_0 & KF_1 & K^2 F_2 \end{bmatrix}^{-1} \begin{bmatrix} \beta \\ \gamma \\ \delta \end{bmatrix}.$$

The object is to ensure that the synthesis matrix is the transpose of the analysis matrix.

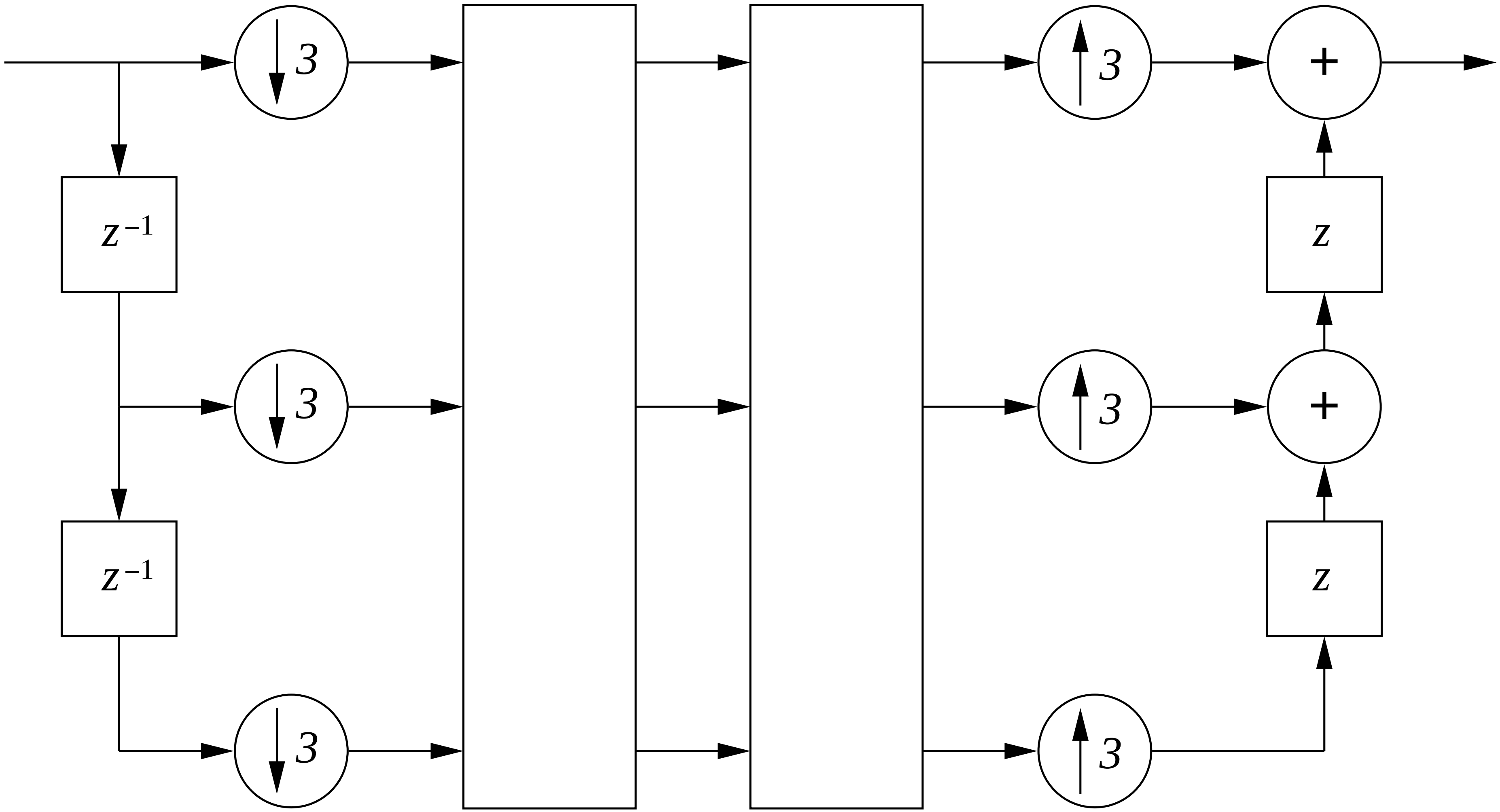

Figure 20. A three-channel filter bank can be constructed that separates the data into three phases.

Triadic Filters: Sequential Orthogonality

Let $\xi(t) \longleftrightarrow \xi(\omega)$ denote the autocorrelation function of any one of the triadic filters together with its Fourier transform. Then, the relevant condition of sequential orthogonality is that $\xi(3t) = 0$ if $t \neq 0$. Define $\lambda = 3\omega$. Then,

$$\begin{aligned}
\xi(3t) &= \frac{1}{2\pi}\int_{-\pi}^{\pi} \xi(\omega) e^{\mathrm{i}\omega(3t)} d\omega \ = \frac{1}{6\pi}\int_{-3\pi}^{3\pi} \xi(\lambda/3) e^{\mathrm{i}\lambda t} d\lambda \\
&= \frac{1}{6\pi}\left\{\int_{-3\pi}^{-\pi} \xi(\lambda/3) e^{\mathrm{i}\lambda t} d\lambda + \int_{-\pi}^{\pi} \xi(\lambda/3) e^{\mathrm{i}\lambda t} d\lambda + \int_{\pi}^{3\pi} \xi(\lambda/3) e^{\mathrm{i}\lambda t} d\lambda\right\} \\
&= \frac{1}{6\pi}\int_{-\pi}^{-\pi} \sum_{j=-1}^{1} \xi([2\pi j + \lambda]/3) e^{\mathrm{i}\lambda t} d\lambda
\end{aligned}$$

Therefore, the condition of orthogonality is equivalent to the condition that the superimposition of the squared gain functions of the three filters constitutes a constant function in the frequency domain:

$$\xi([-2\pi/3] + \omega) + \xi(\omega) + \xi([(2\pi/3] + \omega) = c.$$

When dilated by a factor of three, the squared gain of each of the filters also constitutes a constant function.

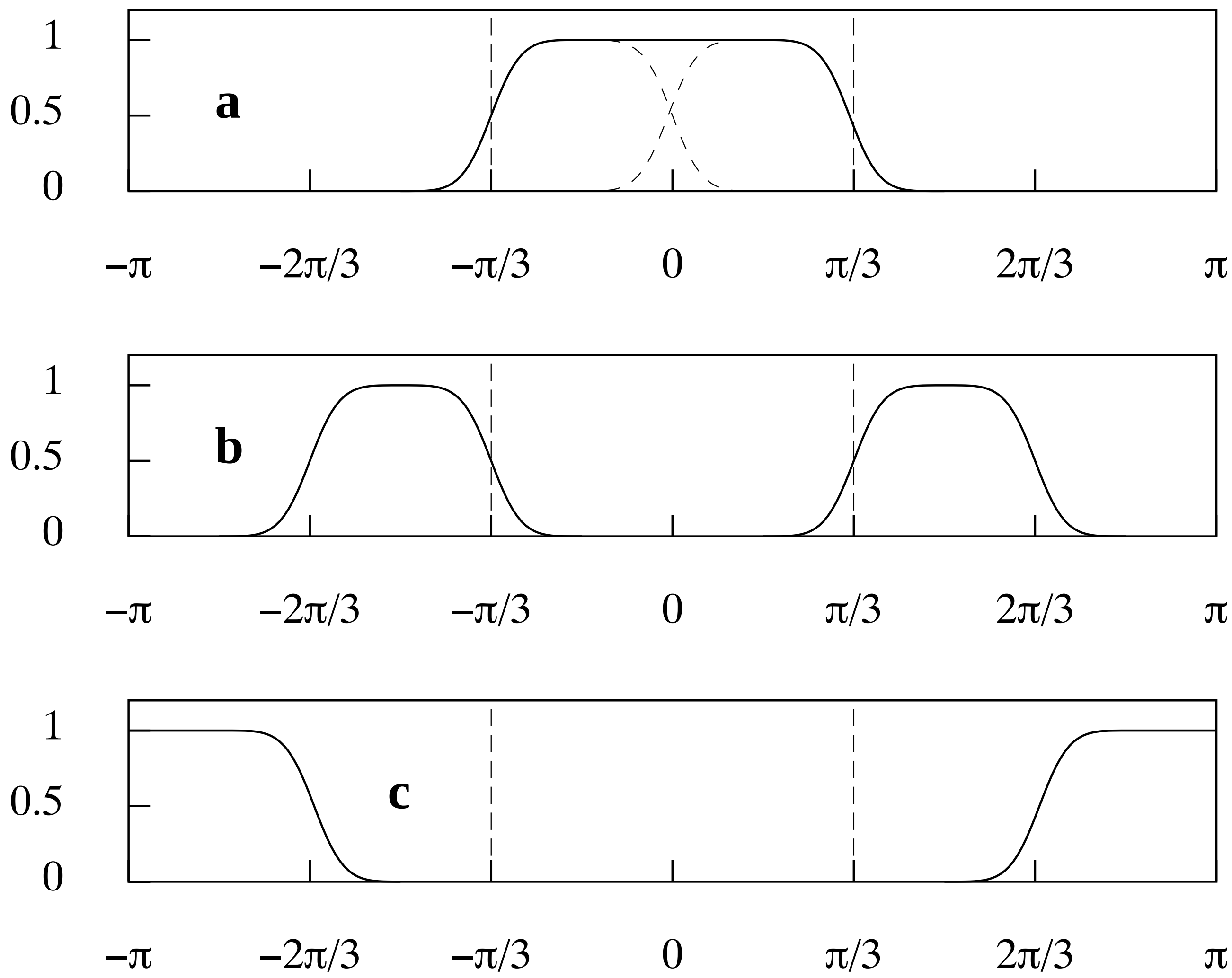

Figure 21. The triadic squared gain functions, which can be superimposed and added to create a constant function.

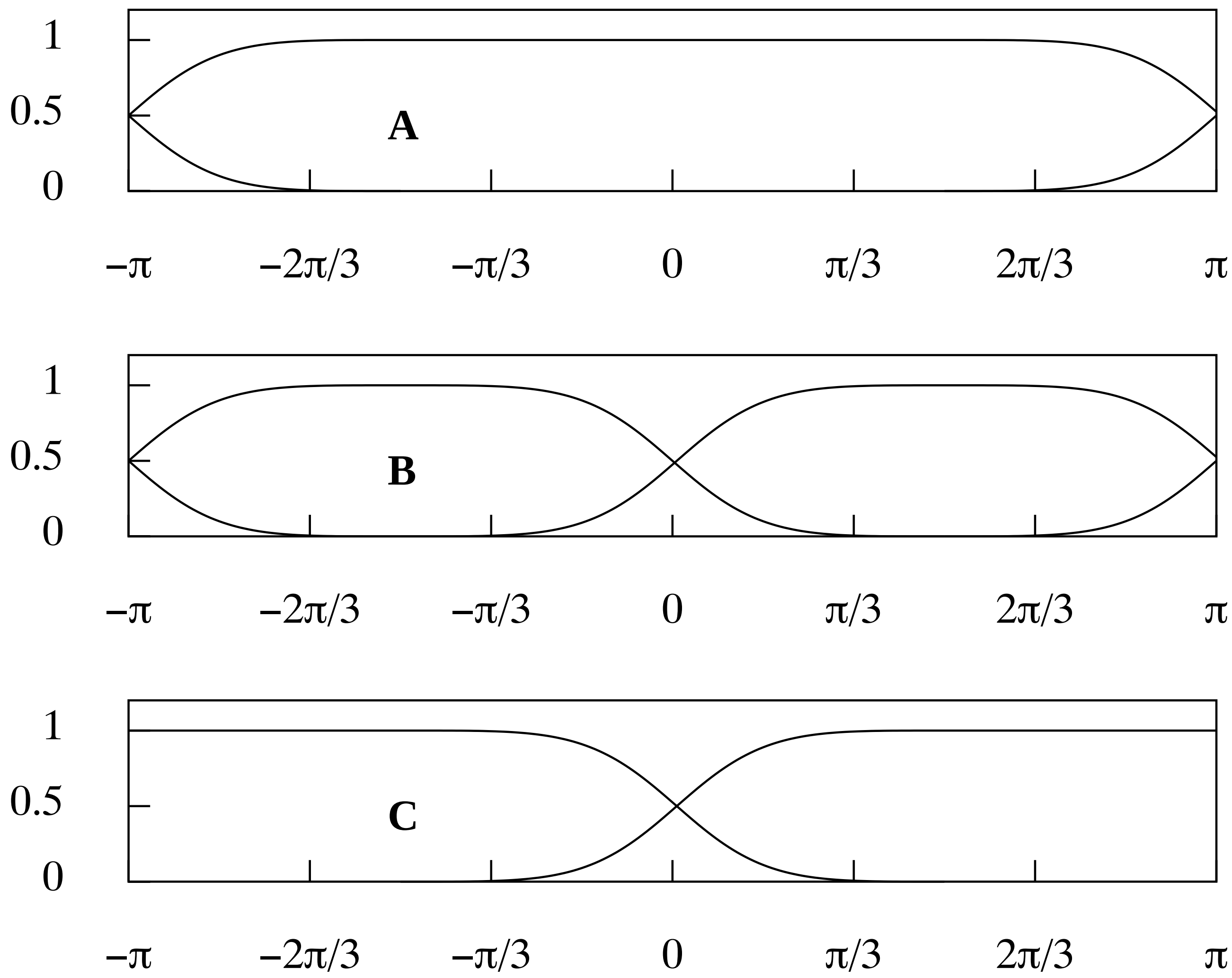

Figure 22. The triadic squared gain functions dilated by a factor of 3. Each of these generates a constant function when the superimposed ordinates are added.